

This work was written as part of one of the author's official duties as an Employee of the United States Government and is therefore a work of the United States Government. In accordance with 17 U.S.C. 105, no copyright protection is available for such works under U.S. Law.

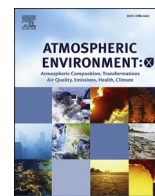
Public Domain Mark 1.0

<https://creativecommons.org/publicdomain/mark/1.0/>

Access to this work was provided by the University of Maryland, Baltimore County (UMBC) ScholarWorks@UMBC digital repository on the Maryland Shared Open Access (MD-SOAR) platform.

**Please provide feedback**

Please support the ScholarWorks@UMBC repository by emailing [scholarworks-group@umbc.edu](mailto:scholarworks-group@umbc.edu) and telling us what having access to this work means to you and why it's important to you. Thank you.



## Modeling air quality in the San Joaquin valley of California during the 2013 Discover-AQ field campaign

Jianjun Chen<sup>a</sup>, Dazhong Yin<sup>a</sup>, Zhan Zhao<sup>a</sup>, Ajith P. Kaduwela<sup>a,b,\*</sup>, Jeremy C. Avise<sup>a,c</sup>, John A. DaMassa<sup>a</sup>, Andreas Beyersdorf<sup>d</sup>, Sharon Burton<sup>e</sup>, Richard Ferrare<sup>e</sup>, Jay R. Herman<sup>f</sup>, Hwajin Kim<sup>g</sup>, Andy Neuman<sup>h,i</sup>, John B. Nowak<sup>e</sup>, Caroline Parworth<sup>g</sup>, Amy Jo Scarino<sup>e</sup>, Armin Wisthaler<sup>j,k</sup>, Dominique E. Young<sup>g</sup>, Qi Zhang<sup>g</sup>

<sup>a</sup> Air Quality Planning and Science Division, California Air Resources Board, Sacramento, CA, USA

<sup>b</sup> Air Quality Research Center, University of California, Davis, CA, USA

<sup>c</sup> Department of Civil and Environmental Engineering, Washington State University, Pullman, WA, USA

<sup>d</sup> Department of Chemistry & Biochemistry, California State University, San Bernardino, CA, USA

<sup>e</sup> NASA Langley Research Center, Hampton, VA, USA

<sup>f</sup> NASA Goddard Space Flight Center, Greenbelt, MD, USA

<sup>g</sup> Department of Environmental Toxicology, University of California, Davis, CA, USA

<sup>h</sup> NOAA Earth System Research Laboratory, Boulder, CO, USA

<sup>i</sup> Cooperative Institute for Research in Environmental Sciences, University of Colorado, Boulder, CO, USA

<sup>j</sup> Institute for Ion Physics and Applied Physics, University of Innsbruck, Innsbruck, Austria

<sup>k</sup> Department of Chemistry, University of Oslo, Oslo, Norway

### ARTICLE INFO

#### Keywords:

CMAQ  
DISCOVER-AQ  
PM<sub>2.5</sub> modeling  
San joaquin valley

### ABSTRACT

The San Joaquin Valley (SJV) of California has one of the nation's most severe wintertime PM<sub>2.5</sub> pollution problems. The DISCOVER-AQ (Deriving Information on Surface Conditions from Column and Vertically Resolved Observations Relevant to Air Quality) field campaign took place in the SJV from January 16 to February 6, 2013. It captured two PM<sub>2.5</sub> pollution episodes with peak 24-h concentrations approaching 70 µg/m<sup>3</sup>. Using meteorological fields generated from WRFv3.6, CMAQv5.0.2 was applied to simulate PM<sub>2.5</sub> formation in the SJV from January 10 through February 10, 2013. Overall, the model was able to capture the observed accumulation of PM<sub>2.5</sub> within the simulation period. The model was able to produce increased concentrations of ammonium nitrate and organic carbon, which are two major components of wintertime PM<sub>2.5</sub> in the SJV. Comparison to measurements made by aircraft showed that there was general agreement between observed and modeled daytime vertical distributions of selected gas and particulate species, reflecting the adequacy of modeled daytime mixing layer heights. Excess ammonia predicted by the model implied that ammonium nitrate formation was limited by the availability of nitric acid, consistent with observations. Evaluation of the ammonium nitrate diurnal profile revealed that the observed morning increase of ammonium nitrate was also evident from the model. This paper demonstrates that the CMAQ model is able to simulate elevated wintertime PM<sub>2.5</sub> formation observed in the SJV during the DISCOVER-AQ 2013 period, which featured both climatic (i.e., 2011–2014 California Drought) and emissions differences compared to a previous large air quality field campaign in the SJV during 1999–2000.

### Introduction

The San Joaquin Valley (SJV or Valley) of California has some of the nation's most severe PM<sub>2.5</sub> (particulate matter with aerodynamic diameter less than 2.5 µm) pollution (American Lung Association,

2018). The region violates the U.S. EPA National Ambient Air Quality Standards (NAAQS) for both 24-h and annual-average PM<sub>2.5</sub> concentrations. Based on the 2012–2014 air quality measurements, SJV's annual and 24-h PM<sub>2.5</sub> design values are 19.1 µg/m<sup>3</sup> and 69 µg/m<sup>3</sup>, respectively, making it the most polluted region in the nation based on

\* Corresponding author. Air Quality Planning and Science Division, California Air Resources Board, 1001 I Street, Sacramento, CA, 95814, USA.

E-mail address: [Ajith.kaduwela@arb.ca.gov](mailto:Ajith.kaduwela@arb.ca.gov) (A.P. Kaduwela).

<https://doi.org/10.1016/j.aeoa.2020.100067>

Received 6 August 2019; Received in revised form 22 January 2020; Accepted 12 February 2020

Available online 15 February 2020

2590-1621/© 2020 The Authors.

Published by Elsevier Ltd.

This is an open access article under the CC BY-NC-ND license

(<http://creativecommons.org/licenses/by-nc-nd/4.0/>).

the U.S. EPA annual  $\text{PM}_{2.5}$  standard and the second most polluted for the 24-h standard. The poor air quality in the Valley results from a confluence of local geography, weather, and proximity to a range of emission sources, including mobile sources, residential wood combustion, commercial cooking, and agricultural activities. Geographically, SJV is surrounded by mountain ranges to the west, east, and south, which helps to trap pollution within the Valley. Climatically, it is characterized by dry, hot summers and cool, humid winters. SJV is home to four million people and is one of the world's most productive agricultural regions (U.S. EPA, 2018). SJV  $\text{PM}_{2.5}$  concentrations have a distinct seasonal cycle (Chow et al., 2006).  $\text{PM}_{2.5}$  concentrations are typically low in summer due to meteorological conditions that increase dilution of emissions and temperatures that are thermodynamically unfavorable for ammonium nitrate formation. In contrast, wintertime stagnant conditions characterized by cold temperatures, calm winds, and a shallow nocturnal inversion layer often lead to elevated  $\text{PM}_{2.5}$  concentrations (Brown et al., 2006; MacDonald et al., 2006; Prabhakat et al., 2017; Watson and Chow, 2002). Because of the severity of the  $\text{PM}_{2.5}$  pollution problem in the SJV, the region's air quality is also among the most studied in the nation (CARB, 2012).

Historically, the most notable study of  $\text{PM}_{2.5}$  pollution in the SJV was the California Regional  $\text{PM}_{10}/\text{PM}_{2.5}$  Air Quality Study (CRPAQS) in 1999–2001 (Solomon and Magliano, 1999; Turkiewicz et al., 2006). The CRPAQS study included monitoring of particulate matter, its precursors, and meteorological parameters at over 100 sites (Chow et al., 2006; Watson and Chow, 2002) in Central California, which includes the SJV. Findings from CRPAQS have dramatically enhanced our understanding of the spatial and temporal distribution, chemical composition, transport and transformation, and emission sources relevant to  $\text{PM}_{2.5}$  pollution in the SJV. Consequently, it has provided a strong scientific foundation for developing air pollution control strategies in the SJV for many years, and in particular for reducing concentrations of ammonium nitrate and organic carbon (OC), which are the two major  $\text{PM}_{2.5}$  components in the Valley (Chen et al., 2014; Ge et al., 2012a, b; Parworth et al., 2017; Young et al., 2016). Over the past 20 years, there have been substantial emission reductions in the SJV. Nitrogen oxides ( $\text{NO}_x$ ), primary  $\text{PM}_{2.5}$ , and volatile organic compounds (VOC) emissions have decreased by 30–40% from 2000 to 2012 (<http://www.arb.ca.gov/ei/emissiondata.htm>; Russell et al., 2010). In addition, California has been under severe drought during 2011–2016, which may have implications for  $\text{PM}_{2.5}$  formation and buildup. Given these changes in emissions and climatic conditions, new field campaigns investigating the spatial and temporal distributions of  $\text{PM}_{2.5}$  and its precursors were needed to better understand recent  $\text{PM}_{2.5}$  pollution in the SJV.

The Deriving Information on Surface Conditions from Column and Vertically Resolved Observations Relevant to Air Quality (DISCOVER-AQ) field campaign, launched by the National Aeronautics and Space Administration (NASA) took place in the SJV from January 16 to February 6, 2013. Its primary goal was to relate column observations using remote sensing techniques to abundance of  $\text{PM}_{2.5}$  and key trace gases such as ozone, nitrogen dioxide, and formaldehyde at the surface ([http://www.nasa.gov/mission\\_pages/discover-aq/science/index.html#.VtTinvkrKM8](http://www.nasa.gov/mission_pages/discover-aq/science/index.html#.VtTinvkrKM8)). During the field campaign, aircraft measurements of  $\text{PM}_{2.5}$  and its precursors were repeatedly made in and above the mixing layers over rural agricultural areas and urban regions in the SJV. They were accompanied by extensive ground-based measurements (e.g., Orozco et al., 2016; Parworth et al., 2017; Young et al., 2016; Zhang et al., 2016). The campaign provided extensive observations of wintertime gases and  $\text{PM}_{2.5}$  throughout the SJV. During the field campaign, the highest 24-h average  $\text{PM}_{2.5}$  concentrations in the SJV were approximately  $70 \mu\text{g}/\text{m}^3$ , which is twice the 24-h national standard of  $35 \mu\text{g}/\text{m}^3$ , and makes the data collected during the DISCOVER-AQ field campaign suitable for updating our conceptual understanding of the formation mechanisms, transport, and emission sources causing elevated wintertime  $\text{PM}_{2.5}$  in the SJV.

Three-dimensional air quality models have been previously used to

simulate  $\text{PM}_{2.5}$  abundance in the SJV (Chen et al., 2009, 2010, 2014; Held et al., 2004; Hu et al., 2010, 2014a,b; Kelly et al., 2014, 2018; Kleeman et al., 2005; Livingstone et al., 2009; Mahmud et al., 2010; Markovic, 2014; Pun et al., 2009; Ying et al., 2008a,b, 2009; Zhang et al., 2010, 2014). However, model simulations of wintertime elevated  $\text{PM}_{2.5}$  episodes in the SJV are challenging, particularly when meteorological fields were generated from prognostic models (Hu et al., 2010, 2014a; Pun et al., 2009; Zhang et al., 2010). High wintertime  $\text{PM}_{2.5}$  concentrations in the SJV are typically dominated by elevated concentrations of ammonium nitrate. Accurately simulated meteorological fields, including wind patterns, mixing layer heights, temperatures, and relative humidity (RH) are crucial for capturing these elevated ammonium nitrate concentrations. However, complex topography makes it challenging to accurately simulate meteorological fields within the SJV (Bao et al., 2008; Hu et al., 2010, 2014a; Zhao et al., 2011). Despite steady emission reductions in the SJV over the past decade, 24-h  $\text{PM}_{2.5}$  design values (defined as the three-year average of the annual 98th percentile of the 24-h average  $\text{PM}_{2.5}$ ) increased substantially during 2011–2014, reversing the previous trend of a 40% decline in design values observed from 1999 to 2010. This reversal of trend in the design value despite continuing emission reductions underscores the importance of modeling wintertime  $\text{PM}_{2.5}$  episodes in the SJV accurately to elucidate effective mitigation strategies.

The main goal of this study is to evaluate the capability of the Weather Research and Forecasting (WRF) and the Community Multi-scale Air Quality (CMAQ) models in simulating  $\text{PM}_{2.5}$  formation and its precursors in the SJV during the DISCOVER-AQ field campaign. While previous model evaluations have been typically limited to ground-based  $\text{PM}_{2.5}$  observations, aircraft measurements from DISCOVER-AQ allow model evaluation of many  $\text{PM}_{2.5}$  precursors (e.g., nitric acid ( $\text{HNO}_3$ ), ammonia ( $\text{NH}_3$ ), and VOCs species) on spatial (e.g., aloft) and temporal scales that were not possible previously.

The modeling system evaluated in this study (i.e., WRF/CMAQ) is the foundation of the State Implementation Plan (SIP) development in the SJV (Chen et al., 2014), and is used to demonstrate how current and/or future control programs will bring the SJV into attainment of  $\text{PM}_{2.5}$  NAAQS. Consequently, it is imperative to fully evaluate, using research-grade measurements, the ability of the WRF/CMAQ modeling system to simulate  $\text{PM}_{2.5}$  and its precursors in the Valley to enhance confidence in a modeling system that is used for policy decision making and regulatory development.

## Modeling episode

The modeled period coincides with the DISCOVER-AQ measurements and covers January 10 through February 10, 2013. Over this period, 24-h  $\text{PM}_{2.5}$  concentrations observed at the ground-based regulatory monitors in the SJV peaked at  $60\text{--}70 \mu\text{g}/\text{m}^3$  in Bakersfield on January 20–23 and again on February 3–4. Prolonged light winds and cooler temperatures from January 16–22 led to enhanced 24-h  $\text{PM}_{2.5}$  on January 20–23 throughout the entire SJV. The second peak on February 3–4 was more pronounced in the southern portion of the Valley than in the central or northern SJV. Light rain was observed in Fresno and Bakersfield on January 10, January 24–27, and February 8–9. Total precipitation in January and February at Fresno and Bakersfield was less than half of the historical mean, which led to reduced removal of  $\text{PM}_{2.5}$  through scavenging and wet deposition, and exacerbated  $\text{PM}_{2.5}$  pollution.

## Air quality and meteorological model configuration

The CMAQ model version 5.0.2 was used to simulate air quality over the modeling period. Gas-phase chemistry was based on the SAPRC07 mechanism (Carter, 2010) and the aerosol dynamics/chemistry was based on the aerosol 6 module. The CMAQ modeling domain covers the entire state of California with a  $4 \times 4 \text{ km}^2$  horizontal grid size and

extends out over the Pacific Ocean to cover the major shipping channels offshore (Fig. 1). Analysis of the modeling is focused on the SJV, which is highlighted in Fig. 1. From south to north, major cities in the SJV included Bakersfield, Visalia, Fresno, Modesto, and Stockton. Among them, Fresno and Bakersfield are the two largest metropolitan regions in the Valley. The CMAQ modeling utilized 30 vertical layers extending from the surface to 100 mb. Chemical boundary conditions were extracted from simulations using the global atmospheric chemical transport Model for Ozone And Related chemical Tracers (MOZART, Emmons et al., 2010; <http://www.acom.ucar.edu/wrf-chem/mozart.shtml>) using the mozart2camx preprocessor (<http://www.camx.com/download/support-software.aspx>). Anthropogenic emissions were based on the most recent California inventory submitted to the U.S. EPA for 2012 and grown to 2013 (<http://www.arb.ca.gov/planning/sip/2012iv/2012iv.htm>). Detailed description of the methodology for emission inventory preparation can be found in CARB (2012) and SJVAPCD (2016). Biogenic emissions were based on a modified version of MEGAN v2.04, which utilized updated emission factor, leaf area, and plant functional type data for California (Misztal et al., 2016).

The WRF model version 3.6 was used to generate meteorological inputs for the CMAQ model. Three two-way nested modeling domains consisting of  $36 \times 36 \text{ km}^2$ ,  $12 \times 12 \text{ km}^2$ , and  $4 \times 4 \text{ km}^2$  horizontal grid sizes were used. The initial and boundary conditions for WRF were based on the North American Regional Reanalysis (NARR) data archived at the National Center for Atmospheric Research (NCAR). In addition, surface and upper air observations obtained from NCAR were used to further refine the analysis data for the outer  $36 \text{ km}$  domain. The WRF simulation was reinitialized every 5 days with a one day spin-up. The physics options (available at [http://www2.mmm.ucar.edu/wrf/users/phys\\_references.html](http://www2.mmm.ucar.edu/wrf/users/phys_references.html)) used included the WRF single-moment 6-class microphysics scheme, the RRTM longwave and the Dudhia short-wave radiation schemes, the revised MM5 Monin-Obukhov surface layer scheme, the 5-layer thermal diffusion scheme, the Yonsei University planetary boundary layer scheme, and the Kain-Fritsch cumulus parameterization. More than a dozen WRF/CMAQ sensitivity runs were conducted involving different physics schemes in the WRF model, and these schemes were selected because the CMAQ simulation based on these configurations yielded the best peak  $\text{PM}_{2.5}$  predictions.

### Observational data

The surface meteorological observations that were used to evaluate model performance included about 100 surface sites located throughout the SJV with temperature and RH measurements and approximately 50 sites with surface wind measurements. Data were downloaded from the California Air Resources Board (CARB)'s Air Quality and Meteorological Information System (AQMISS2) database (<http://www.arb.ca.gov/aqmiss2/metselect.php>). In addition, daytime mixing layer (ML) heights were derived by NASA's Langley Research Center (LaRC) based on aerosol backscattering measurements made from LaRC's airborne High Spectral Resolution Lidar (HSRL; Brooks et al., 2003; Scarino et al., 2014). The derived ML data were used to evaluate the boundary layer (BL) height from the meteorology-chemistry interface processor (MCIP; Otte and Pleim, 2010), which converts WRF outputs to meteorological inputs for CMAQ. The availability of ML height estimates in the SJV is important because they play a critical role in high  $\text{PM}_{2.5}$  episodes in the SJV (MacDonald et al., 2006). Aircraft measured temperature and RH were also used to evaluate model predictions of meteorological parameters aloft. Vertical winds measured by a wind profiler in Visalia were used to evaluate simulated vertical wind profiles.

Surface air quality observations included those for key gases,  $\text{PM}_{2.5}$  mass, and  $\text{PM}_{2.5}$  composition. Measured ozone ( $\text{O}_3$ ) and nitrogen dioxide ( $\text{NO}_2$ ) mixing ratios were obtained from 25 to 16 ground-based monitors located in the SJV, respectively. Daily average  $\text{PM}_{2.5}$  concentrations were obtained from 20 monitoring stations with Beta Attenuation Monitoring (BAM) instruments. These are preferred over the filter-based  $\text{PM}_{2.5}$  measurements using the federal reference method (FRM) because the latter measurement is typically not made every day. In addition, observations of  $\text{PM}_{2.5}$  compositions were obtained from the four speciation sites (i.e., Bakersfield, Fresno, Modesto, and Visalia) in the SJV. Typically, speciation measurements were made every three or six days at these sites. Given that ammonium nitrate is the most abundant  $\text{PM}_{2.5}$  component, highly time resolved ammonium nitrate measurement from an aerosol mass spectrometer (AMS) deployed at Fresno (Young et al., 2016) was also used to evaluate the modeled diurnal cycle of ammonium nitrate.

In addition to the surface measurements, the NASA P3B and B200 aircraft made multiple flights in the SJV during the field campaign. Fig. 1 shows the flight track for the January 20 flight. Other flights shared similar tracks. Here we present model comparison focused on

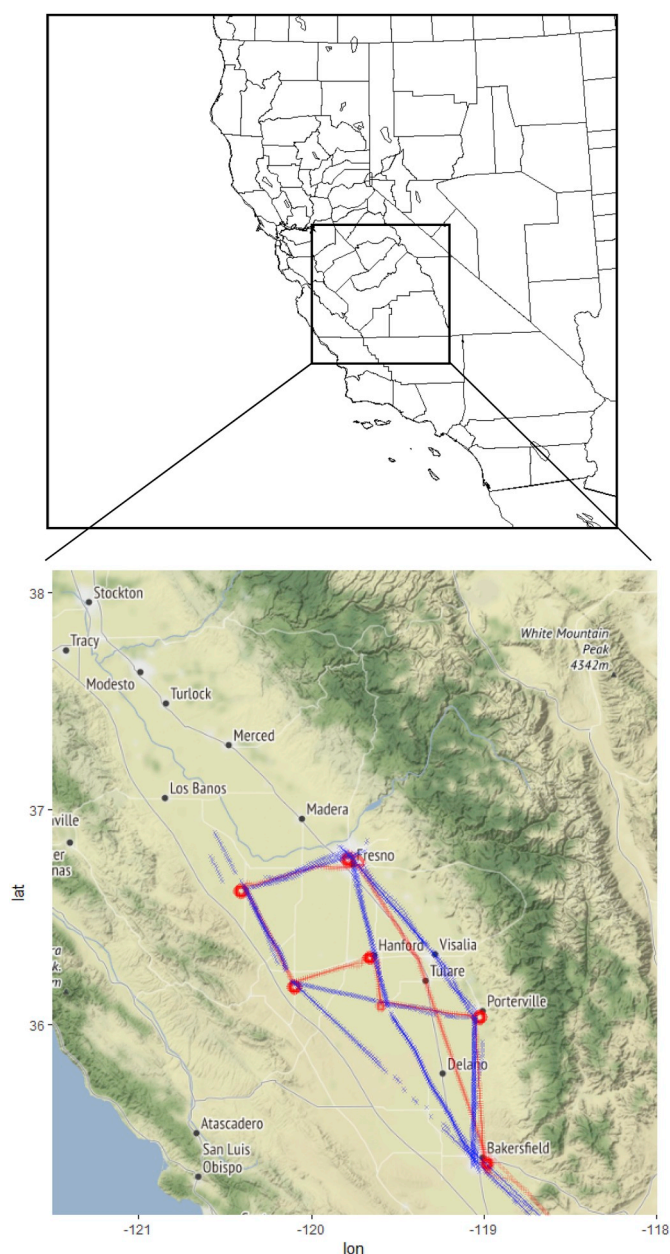


**Fig. 1.** Modeling domain (top), major cities in the SJV and the NASA P3B (in red line) and B200 (in blue line) flight tracks on January 20 (bottom). The circles in the flight track are vertical profiles from approximately 100 m to 2500 m above the ground. (For interpretation of the references to colour in this figure legend, the reader is referred to the Web version of this article.)



measurements from the January 20 flight since it coincided with high  $\text{PM}_{2.5}$  pollution. Comparisons were also made for other flights (supplementary). Of particular importance, measurements in the planetary BL near major urban and agricultural areas allowed for model performance evaluations of vertical pollutant distributions in these critical areas. Comparisons focused on the following species:  $\text{NO}$ ,  $\text{NO}_2$ , reactive odd nitrogen ( $\text{NO}_y$ ), and  $\text{O}_3$  measured by a 4-channel chemiluminescence instrument, total  $\text{HNO}_3$  (gas + particle phase) measured by the laser induced fluorescence method, selected VOC species (i.e., formaldehyde ( $\text{HCHO}$ ) measured by difference frequency absorption spectroscopy, acetaldehyde, benzene, and toluene measured by the proton-transfer-reaction time-of-flight mass spectrometer (PTR-MS)), ammonia ( $\text{NH}_3$ ) measured by a cavity ring down spectrometer (CRDS), and particulate

ammonium and nitrate measured by a particle into liquid sampler (PILS). Ammonia was also measured by a PTR-MS, which has shorter response time than CRDS. Because CRDS has better signal-to-noise ratio (Sun et al., 2015), CRDS measured  $\text{NH}_3$  was used in the paper. For all aircraft data, 1 second merged observational data were downloaded from the NASA field campaign website (<http://www-air.larc.nasa.gov/cgi-bin/ArcView/discover-aq.ca-2013?MERGE=1> and <https://doi.org/10.5067/Aircraft/DISCOVER-AQ/Aerosol-TraceGas>).

Given the importance of nitrogen oxides ( $\text{NO}_x$ ) to the formation of wintertime ammonium nitrate in the SJV (Chen et al., 2014; Pusede and Cohen, 2012; Pusede et al., 2016), it is crucial to evaluate the  $\text{NO}_x$  emissions in the SJV. NASA deployed ground-based Pandora systems (Herman et al., 2009) at 12 locations in the SJV to measure column  $\text{NO}_2$

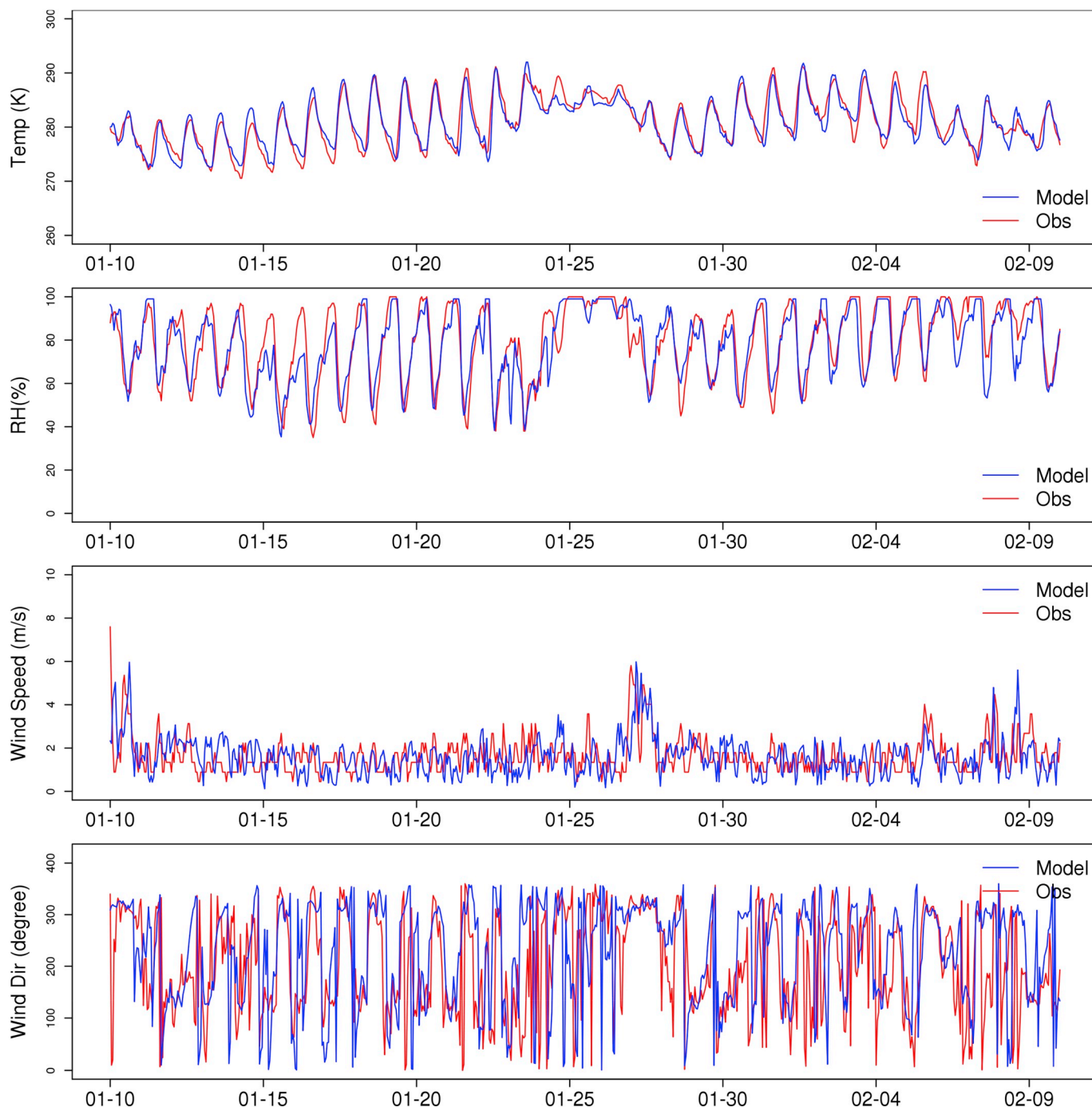


Fig. 2. Comparison of observed and modeled surface meteorological parameters at the Visalia airport.

concentrations in the SJV. These data were also used to evaluate modeled column  $\text{NO}_2$  predictions.

## Results

### Meteorological parameters

The WRF model output is compared with measured surface meteorological conditions in the SJV. Fig. 2 compares modeled and observed temperature, RH, wind speed, and wind direction at the Visalia airport. Overall, there is good agreement between observed and modeled parameters. SJV generally has high RH in winter, particularly at night. Accurately predicting RH is important for simulating ammonium nitrate as higher RH is conducive to the heterogeneous formation of nitric acid at night (Davis et al., 2008) and nighttime heterogeneous nitric acid formation is a major pathway for the production of nitric acid in the SJV (Pusede et al., 2016). The WRF model was able to accurately simulate the diurnal trend and day-to-day variability in both temperature and RH at the Visalia airport. In addition, WRF was able to reproduce the local effects from the various weather systems that passed through the region during the study period. In particular, the model captured the light winds during January 12–23 and January 28–February 4, associated

with high pressure systems, as well as the effect that a low pressure system had on temperature, RH, and winds as it passed through the region January 25–27.

A summary of model performance at all ground stations is shown in Fig. S1. For temperature, RH, and wind speed, mean observations, mean model predictions, mean fractional bias (MFE), and mean fractional errors (MFE) were calculated for each parameter at each site (Boylan and Russell, 2006). Box plots were used to show the range of those statistics across different stations. On average, RH is somewhat over predicted with a median fractional bias of 0.03. Wind speed is over predicted with a median fractional bias of 0.15, and temperature is slightly over predicted with a median fractional bias of 0.01. Median fractional errors of RH, wind speed, and temperature are 0.16, 0.56, and 0.01, respectively. Over prediction of calm wind speed in the SJV by prognostic meteorological models has been documented previously (Hu et al., 2010) and further improvement in model predictions of calm winds is warranted.

Fig. 3 shows the comparison of vertical distributions of temperature, RH, and wind speed and direction. The vertical distributions for temperature and RH represent average vertical distributions based on measurements from the NASA P3B flight on Jan 20. In general, there is agreement between modeled and observed temperature and RH.

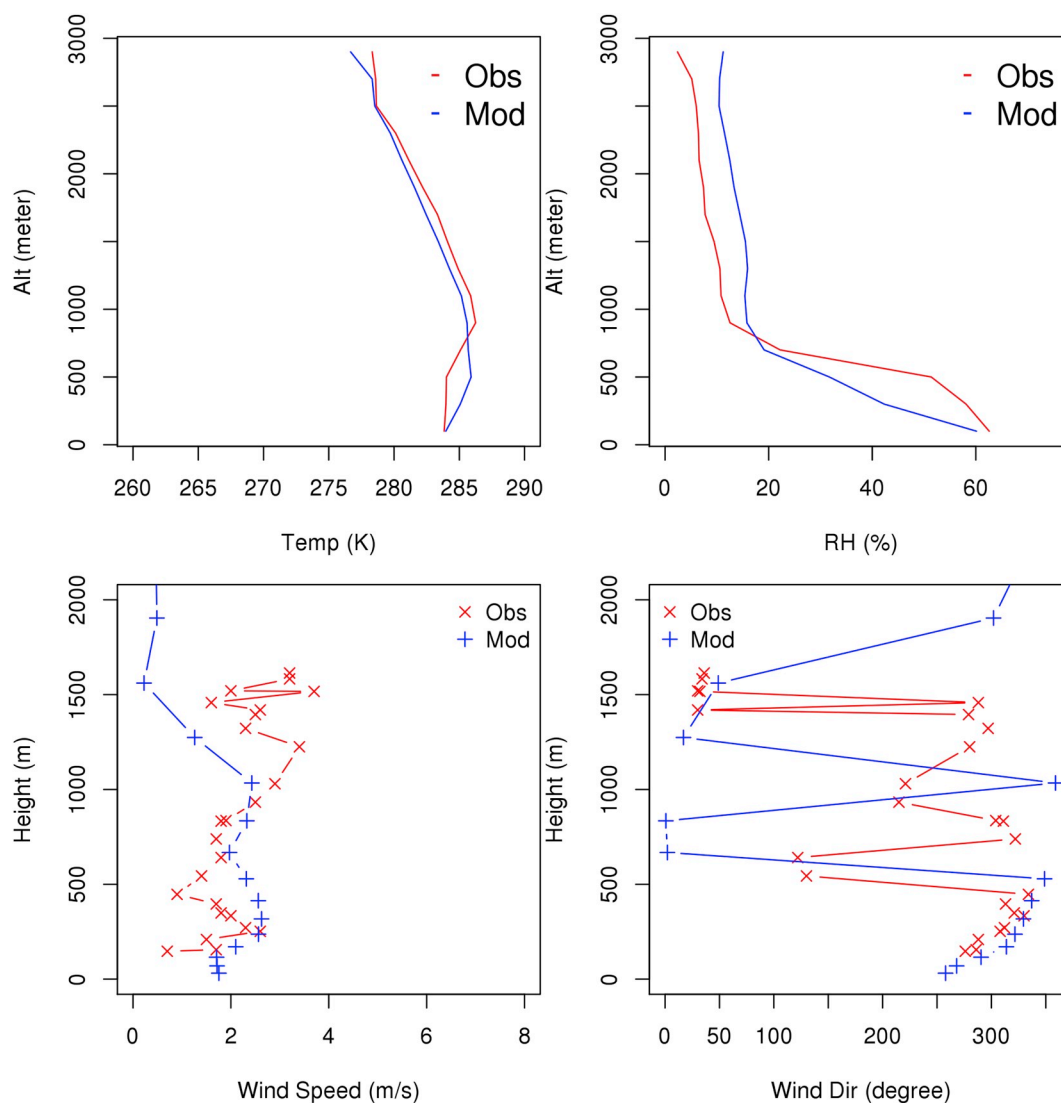


**Fig. 3.** Comparison of average vertical temperature and RH distributions based on the NASA P3B flight on Jan 20 (Top); Comparison of vertical profiles of wind speed and direction at 11 a.m. (PST) on Jan 20 based on measurement from a wind profiler near Visalia (Bottom).

Temperature is slightly over-predicted in the lower portion of the atmosphere, with a corresponding under-prediction in RH. Based on second-by-second comparison for the entire field campaign, the mean fractional bias in temperature and RH is 0.001 and 0.07, respectively, and the mean fractional error in temperature and RH is 0.005 and 0.35, respectively. Aircraft measured wind speeds during spirals were frequently unrealistically high, therefore modeled wind speed distribution was instead compared to the measurements from a 915-MHz radar wind profiler located near Visalia. The bottom two plots in Fig. 3 shows a sample comparison for vertical distributions of wind speed and direction at 11am (PST) on Jan 20. Modeled wind speed is close to observed speed, which is within the range of 1–3 m/s and is typical during winter PM<sub>2.5</sub> episode days in the SJV (MacDonald et al., 2006). On average, modeled wind speed is within 20% of observed values below 2 km on January 20. Modeled wind direction also showed general agreement with the observed direction. Both showed northwesterly winds in the lowest 500 m. Between 500 and 1000 m, the model showed northerly winds, while observations showed northwesterly winds. Above 1000 m, the model showed northeasterly winds, while observations showed winds ranging between northwesterly to northeasterly. Comparison of the wind prediction in terms of observed and predicted wind roses for the entire modeling period is shown in Figs. S2, S3, and S4 for winds below 500 m, 500–1000 m, and 1000–2000 m, respectively. The comparison shows that the WRF model reproduced key features of the observed wind patterns including the occurrence of low wind conditions and high winds from a predominantly northwesterly direction.

Fig. 4 shows the comparison between modeled planetary BL height and derived ML height from the HSRL measurement on January 20. The location of Bakersfield and Fresno overpasses are also marked on the plot. Conceptually, these two heights are not exactly the same as the CMAQ BL height is based on thermodynamic profiles and the HSRL ML height is based on aerosol backscatter profiles (Scarino et al., 2014). However, the evaluation is still valuable to ensure that BL height is not over-estimated in the model. Shallow BL height is one of the major reasons for elevated PM<sub>2.5</sub> concentrations in the SJV. Over prediction of BL height can lead to under prediction of PM<sub>2.5</sub> concentrations. In the morning, the modeled BL height (approximately 50–100 m) is generally much smaller than the HSRL derived ML height (100–600 m). In the afternoon, the modeled ML height (200–400 m) is closer to HSRL ML height (400–600 m), although modeled ML height is still smaller than the HSRL derived ML height. The modeled BL height is consistent with

observations from the CRPAQS study, which shows that nighttime and early morning BL height was approximately 50–100 m and afternoon ML height was approximately 400 m on elevated PM<sub>2.5</sub> days (MacDonald et al., 2006). The discrepancy between modeled BL height and the derived ML heights is partially due to different definitions. A further examination of the predicted aerosol mass vertical distributions from CMAQ indicated that vertically, the steepest aerosol mass gradient also generally occurs at approximately 300–400 m above the ground for both the morning and the afternoon flight tracks. Comparisons made for other days (i.e., Jan 16, 18, 21, 22) showed similar results as Jan 20. For Jan 30, 31 and Feb 1, 4, ML heights were higher in both the model and from the HSRL measurement than those of Jan 20. This comparison demonstrated that the BL height in the current modeling system was appropriate in the SJV.

#### Chemical species at ground stations

Fig. 5 compares time series of hourly observed and modeled O<sub>3</sub> and NO<sub>2</sub> mixing ratios at Fresno. Diurnal variations in observed O<sub>3</sub> were captured by the model. Both observed and modeled peak O<sub>3</sub> mixing ratios are generally below 50 ppb, reflecting low photochemical ozone formation in the winter (Chen et al., 2014; Ying et al., 2008). Nighttime O<sub>3</sub> is over predicted, which is also common in previous studies (Chen et al., 2014; Zhang et al., 2010). There is also general agreement between observed and predicted NO<sub>2</sub> mixing ratios. On average, NO<sub>2</sub> is somewhat over predicted at this site by approximately 10%. Fig. S5 shows box and whisker plots of mean observed and modeled mixing ratios as well as mean fractional bias (MFB) and mean fractional errors (MFE) for model predictions of O<sub>3</sub> and NO<sub>2</sub>, respectively. The plots are based on hourly observations and model predictions at approximately 20 monitors in the SJV. Model performance for these two species is also comparable to previous studies (Chen et al., 2014; Ying et al., 2008a). On average, observed NO<sub>2</sub> mixing ratios for all these sites are roughly 30% below average NO<sub>2</sub> observed at approximately 70 sites in Central California (including SJV) during December 25–31, 2000 (Zhang et al., 2010). This reduction primarily reflects the large NO<sub>x</sub> emission reductions in the SJV from 2000 to 2013.

Fig. 6 shows comparisons of observed (using beta attenuation monitoring (BAM)) and modeled 24-h average PM<sub>2.5</sub> concentrations at four individual sites (i.e., Modesto, Visalia, Fresno, and Bakersfield). In addition, the daily mean of 20 sites located throughout the SJV is also

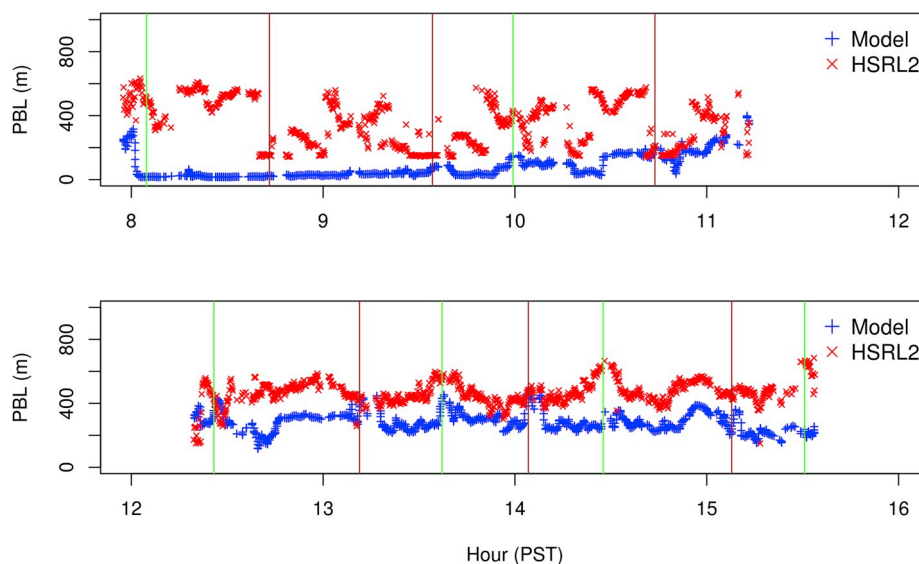


Fig. 4. Comparison between modeled boundary layer height and observed mixing layer height derived from the NASA HSRL aerosol measurements (The vertical green line represents measurement over Bakersfield and the brown line represents measurement over Fresno). (For interpretation of the references to colour in this figure legend, the reader is referred to the Web version of this article.)

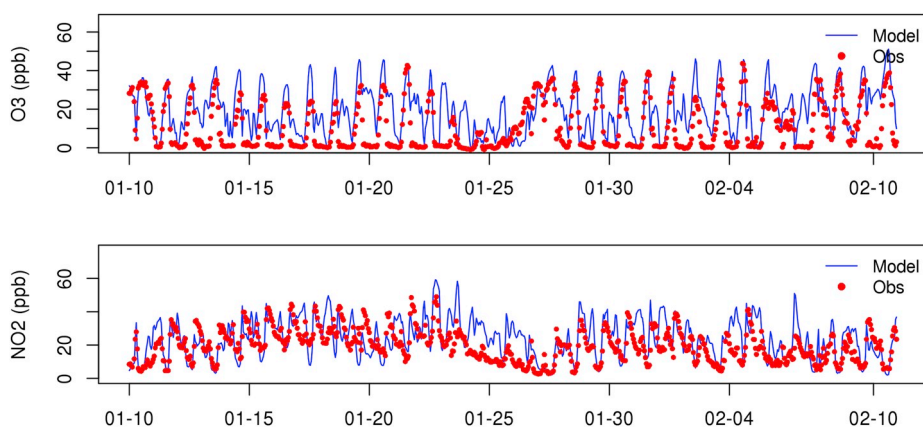


Fig. 5. Comparison of observed and modeled hourly  $O_3$  and  $NO_2$  mixing ratios at Fresno.

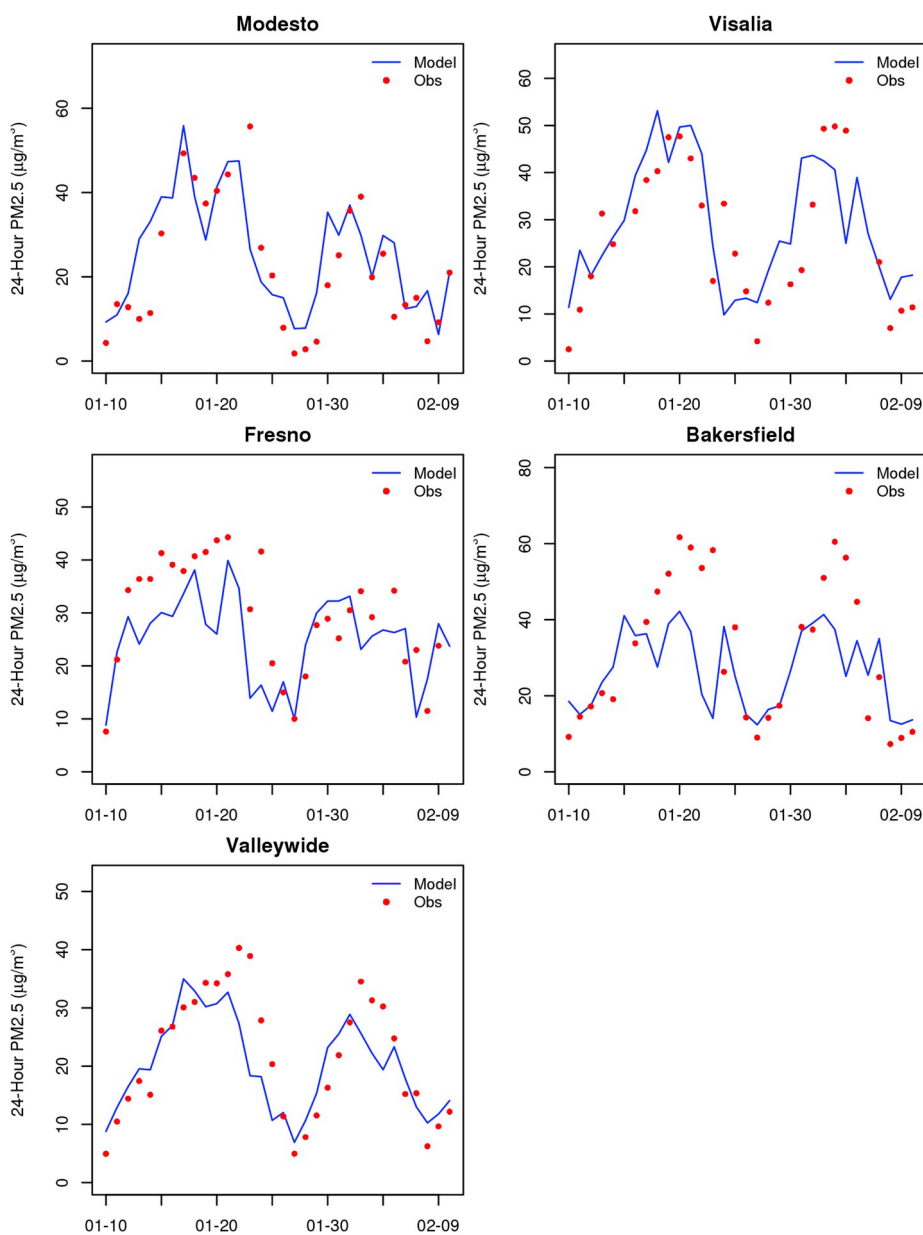


Fig. 6. Time series of observed (BAM) and modeled 24-h  $PM_{2.5}$  concentrations during DISCOVER-AQ.



shown and is termed as valley-wide. Observed PM<sub>2.5</sub>, averaged across the valley, showed gradual accumulation during January 10–23 and again during January 28–February 4. Modeled PM<sub>2.5</sub> generally showed a similar trend. However, peak PM<sub>2.5</sub> concentrations were under predicted. Modeled PM<sub>2.5</sub> concentrations started to show a decrease after January 21 while observed PM<sub>2.5</sub> peaked on January 22–23. The difference in the timing of peak PM<sub>2.5</sub> concentrations is likely due to limitations in the simulated meteorological fields. Similarly for the second episode, modeled PM<sub>2.5</sub> peaked on February 2, while observed PM<sub>2.5</sub> peaked on February 3. Overall, model performance was better in Modesto, which is in the northern SJV, and deteriorated somewhat in Bakersfield, which is located in the southern SJV. The decrease in model performance in the southern SJV is likely due to the area's complex topography compared to the northern SJV, combined with uncertainties associated with emission sources such as dairies and oil fields (Cai et al., 2016). The southern end of the SJV is surrounded by mountains on three sides, and the influence of mixing and transport processes in the area is more complex than in the central or northern SJV (Pusede et al., 2016). Table S1 in the supplementary material shows the 24-h PM<sub>2.5</sub> model performance statistics for all the 20 sites in the SJV. Overall model performance is consistent with other studies (Chen et al., 2014; Simon et al., 2012). The Huron site showed the largest negative fractional bias. Huron is a rural city located far from the major emission source region (i. e., along highway 99). Comparisons of modeled PM<sub>2.5</sub> species with measurements from the NASA P3B indicated that one of the reasons for the large negative bias in Huron is the under prediction of ammonium nitrate (e.g., on Jan 22). The under prediction at Huron is likely due to a combination of inadequate transport in the model or limitations in the characterization of local emission sources.

Table 1 shows the average observed and modeled PM<sub>2.5</sub> species at four sites (i.e., Modesto, Visalia, Fresno, and Bakersfield) in the SJV. Model performance in terms of MFB and MFE for each species is also shown. For the majority of species, model performance meets the criteria established in Boylan and Russell (2006), Eder and Yu (2006), Simon et al. (2012), US EPA (2007) and Yu et al. (2018). Both observations and model results showed that wintertime PM<sub>2.5</sub> in the SJV was dominated by ammonium nitrate and OC. On average, the model over-predicted ammonium nitrate except at Bakersfield. At Bakersfield, under prediction of peak PM<sub>2.5</sub> is caused to a greater degree by under

prediction of ammonium nitrate. Historically, ammonium nitrate predictions at Bakersfield have been more difficult than other regions in SJV (Chen et al., 2014; Kelly et al., 2018; Ying et al., 2008) due to a combination of factors such as more complex topography in the southern portion of the SJV (Kelly et al., 2018) and uncertainties in emissions from sources such as dairies and oil fields (Cai et al., 2016). OC concentrations are generally under predicted, similar to previous studies in the region (Chen et al., 2010, 2014). Improvement in the primary organic aerosol emissions inventory, particularly those associated with residential wood burning, and enhanced secondary organic aerosol (SOA) formation in the model are likely needed to reduce the negative bias in predicted OC (Chen et al., 2010; Young et al., 2016). Finer model grid resolution may also help as OC is dominated by primary emissions and SJV has a very shallow BL at night and early in the morning. Contributions from sulfate and EC to PM<sub>2.5</sub> are smaller and model predictions are generally reasonable.

### Vertical distributions of chemical species

Figs. 7–9 show the observed and modeled daytime vertical distributions of concentrations for key gases and PM<sub>2.5</sub> species based on P3B measurements on Jan 20. Fig. 7 shows the average values from the entire track of the P3B flight. Figs. 8 and 9 compare the vertical profiles based on P3B spirals at Fresno and Porterville, respectively. On Jan 20, both observations and model predictions showed high PM<sub>2.5</sub> concentrations in the SJV. Comparisons of observed and modeled vertical distributions of species for all other flights are shown as Figs. S6–S14 in the supplementary material. Vertical distributions were created by binning both observations and model predictions into 200 m intervals based on altitude above sea level. For simplicity, average values of each bin are shown for both observations and model predictions. Using median instead of mean values for each bin showed similar characteristics. Model predictions corresponding to the second by second observations were linearly interpolated both horizontally as well as vertically from the gridded CMAQ outputs.

Fig. 7 shows that on average, there is general agreement in the modeled and observed vertical distributions of NO, NO<sub>2</sub>, total HNO<sub>3</sub> (gas + aerosol phases, or g + p), and NO<sub>y</sub>. The measured HNO<sub>3</sub> (g + p) included both gaseous and particulate nitrate, therefore modeled

**Table 1**  
Model performance statistics for 24-h average concentrations of PM<sub>2.5</sub> chemical species.

Site	Species	Number of samples	Avg Obs. (µg/m <sup>3</sup> )	Avg Mod. (µg/m <sup>3</sup> )	Mean Bias (µg/m <sup>3</sup> )	Mean Error (µg/m <sup>3</sup> )	MFB <sup>b</sup> (%)	MFE <sup>b</sup> (%)
Fresno	PM <sub>2.5</sub> <sup>a</sup>	11	27.5	24.8	−2.7	9.4	<b>2</b>	<b>38</b>
	Ammonium	11	2.1	2.8	0.8	1.3	<b>49</b>	<b>65</b>
	Nitrate	11	7.3	9.5	2.1	4.1	<b>36</b>	<b>58</b>
	Sulfate	11	0.7	0.9	0.2	0.3	<b>24</b>	<b>43</b>
	OC	9	6.7	4.7	−2.0	2.4	<b>−25</b>	<b>40</b>
	EC	9	1.8	1.7	0.0	0.5	<b>7</b>	<b>33</b>
	PM <sub>2.5</sub>	6	26.4	28.7	2.4	5.9	<b>21</b>	<b>29</b>
Visalia	Ammonium	6	2.7	4.1	1.4	1.5	<b>69</b>	<b>71</b>
	Nitrate	6	9.4	13.9	4.5	4.5	<b>57</b>	<b>57</b>
	Sulfate	6	0.9	0.7	−0.2	0.3	<b>−15</b>	<b>38</b>
	OC	6	6.0	4.1	−2.0	2.3	<b>−29</b>	<b>41</b>
	EC	6	1.2	1.4	0.2	0.3	<b>31</b>	<b>36</b>
	PM <sub>2.5</sub>	7	30.7	23.5	−7.2	13.2	<b>0</b>	<b>45</b>
	Ammonium	7	3.4	2.3	−1.1	2.2	<b>26</b>	<b>82</b>
Bakersfield	Nitrate	7	10.9	7.9	−2.9	5.7	<b>6</b>	<b>57</b>
	Sulfate	7	1.0	0.6	−0.5	0.6	<b>−22</b>	<b>48</b>
	OC	7	5.2	5.9	0.7	2.2	<b>23</b>	<b>46</b>
	EC	7	1.4	1.9	0.6	0.6	<b>43</b>	<b>44</b>
	PM <sub>2.5</sub>	6	24.2	21.6	−2.6	5.5	<b>5</b>	<b>39</b>
	Ammonium	6	1.0	2.3	1.3	1.3	<b>91</b>	<b>91</b>
	Nitrate	6	7.2	7.8	0.7	1.1	<b>11</b>	<b>31</b>
Modesto	Sulfate	6	0.8	0.8	0.0	0.2	<b>27</b>	<b>45</b>
	OC	4	8.4	5.4	−2.9	3.5	<b>−21</b>	<b>46</b>
	EC	4	1.8	1.8	0.0	0.4	<b>19</b>	<b>31</b>

<sup>a</sup> PM<sub>2.5</sub> was measured based on the gravimetric method on selected days. Therefore, they are different from daily BAM measurements.

<sup>b</sup> Statistics meeting the model performance criteria established in Boylan and Russell (2006) is highlighted in bold.

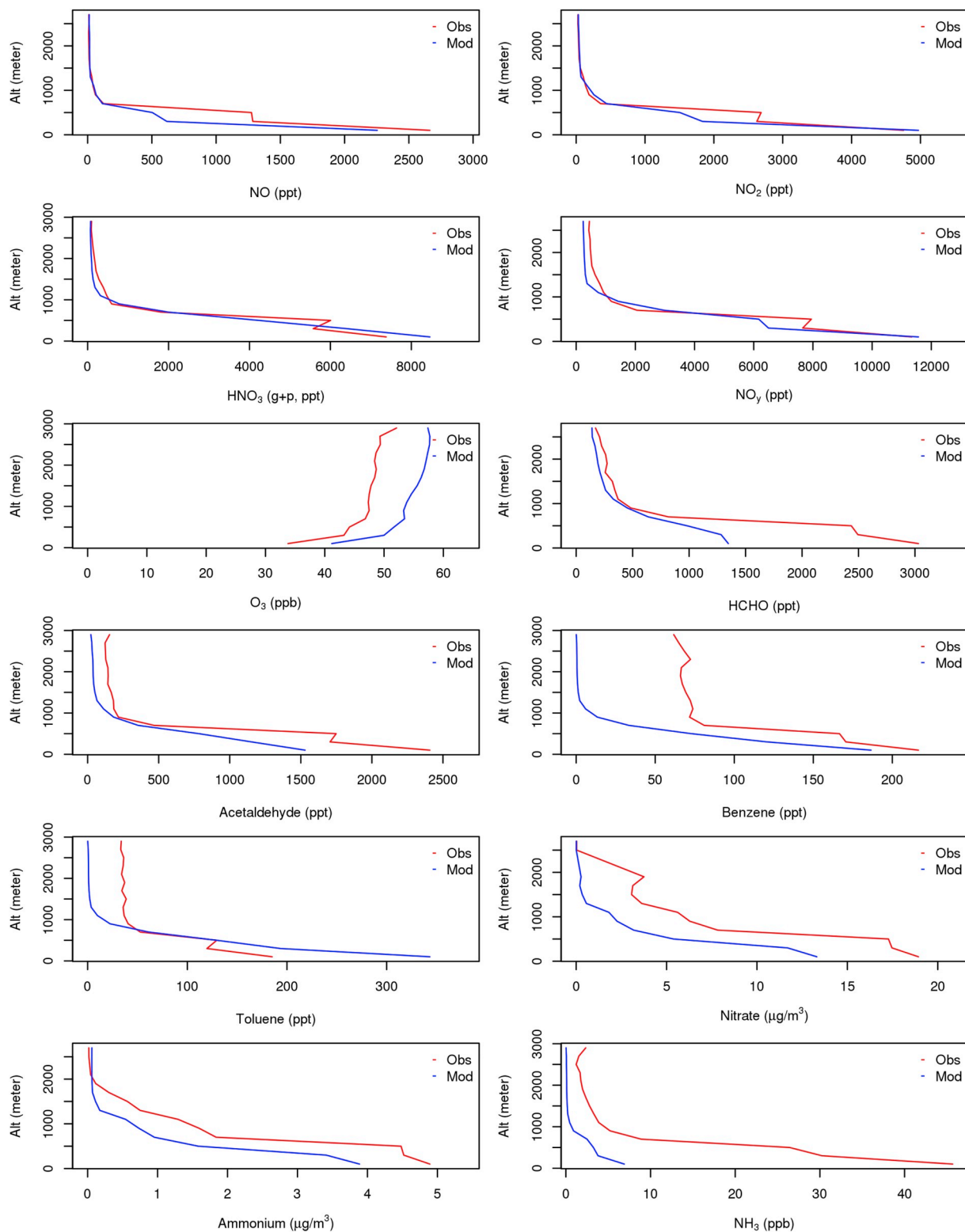


Fig. 7. Comparison of observed and modeled average vertical distributions of key species based on NASA P3B flight on Jan 20.

particulate nitrate was converted to mixing ratio and was added to the modeled gaseous  $\text{HNO}_3$  to calculate the total predicted  $\text{HNO}_3$ . In addition, the measured  $\text{NO}_y$  likely had some contribution from aerosol nitrate and based on Kelly et al. (2018), an additional 20% from the modeled nitrate was added to the gaseous  $\text{NO}_y$  to account for this contribution.  $\text{HNO}_3$  is a key precursor to ammonium nitrate, so evaluating modeled  $\text{HNO}_3$  is critical. The comparison of modeled to observed

$\text{HNO}_3$  showed that on average,  $\text{HNO}_3$  predicted by the model was close to observations within the BL. For these species, in the daytime, mixing ratios dropped to very low values above approximately 600 m (GPS altitude, or 500 m above the ground in the SJV). Both observed and modeled  $\text{O}_3$  mixing ratios were lower near the surface due to titration by fresh  $\text{NO}$  emissions. Mixing ratios of  $\text{O}_3$  aloft represents background levels since there is only minimal local photochemical activity during

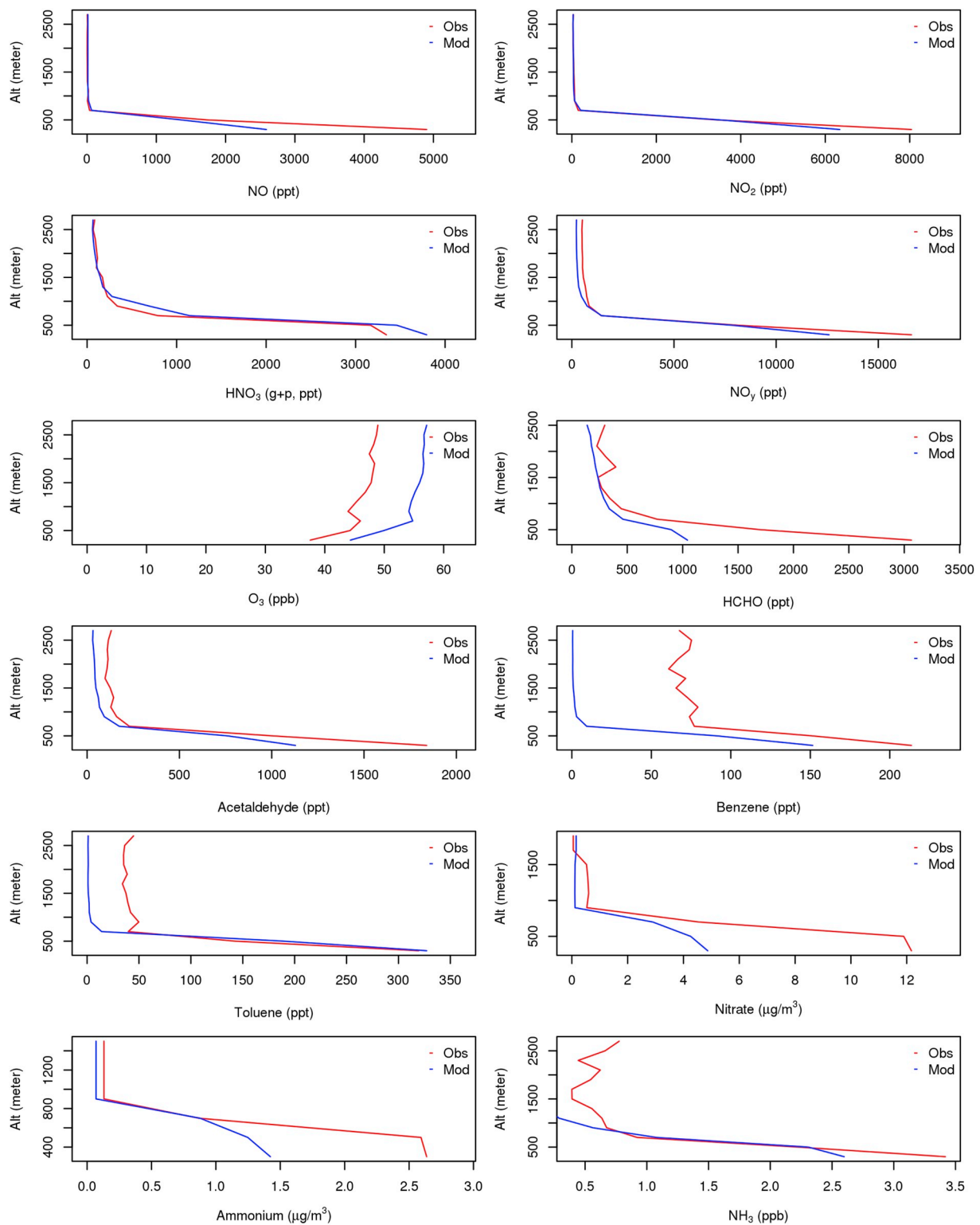


Fig. 8. Comparison of observed and modeled vertical distributions of key species at Fresno based on NASA P3B flight at 12pm and 14pm on Jan 20.

winter months. On average  $O_3$  mixing ratios are over predicted most likely related to potential overestimation of  $O_3$  from boundary conditions as well as the CMAQ model version. Sensitivity analysis with CMAQv5.0.1 (not shown) showed smaller bias. A few VOC species were also examined here because of their potential role in photochemical reactions. Formaldehyde and acetaldehyde in the BL were also under predicted. Potential improvement is needed regarding emissions of the oxygenated VOCs and their precursors (Luecken et al., 2012),

particularly from sources such as biomass burning (Young et al., 2016), dairy, and oil fields in the SJV (Cai et al., 2016). Benzene and toluene are two species characteristic of automobile sources (Pollack et al., 2013). Benzene was slightly under predicted while toluene was over predicted by roughly a factor of two in the BL. Near the surface, modeled nitrate and ammonium is approximately  $4 \mu\text{g}/\text{m}^3$  and  $1 \mu\text{g}/\text{m}^3$  lower than observations, respectively. The vertical distributions of nitrate and ammonium is smeared by a longer sampling time period (i.e., 240 s or a

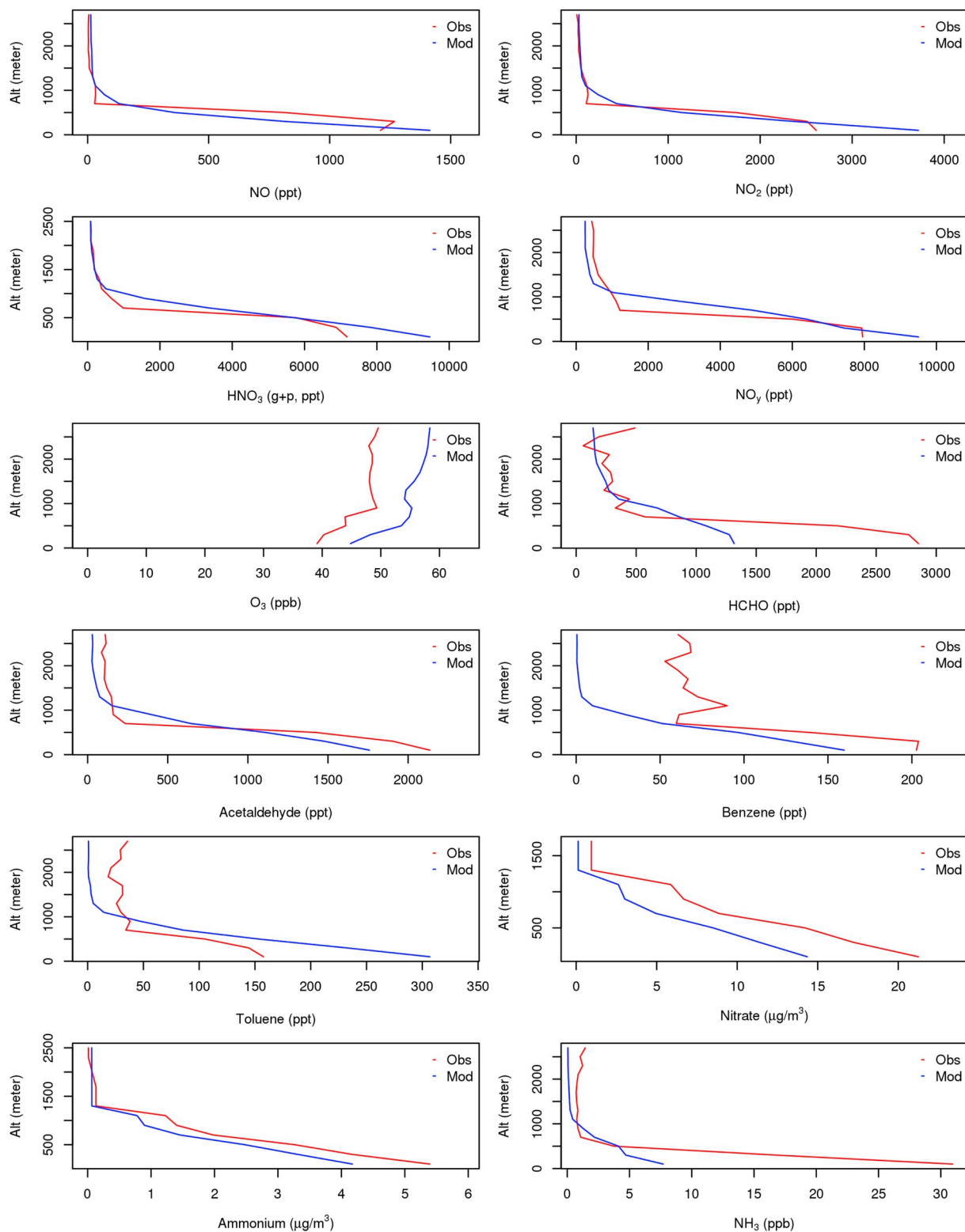


Fig. 9. Comparison of observed and modeled vertical distributions of key species at Porterville based on NASA P3B flight at 10am and 12pm on Jan 20.

few hundred meters vertically dependent on plane's ascending/descending rates) that can mix air from different altitudes.  $\text{NH}_3$  mixing ratios were under predicted by the model. However while  $\text{NH}_3$  was under-predicted, it was found that there was generally enough modeled  $\text{NH}_3$  to fully neutralize nitric acid and sulfate in the model, consistent with observations as well as from previous field measurements (e.g., Lurmann et al., 2006; Markovic et al., 2014; Parworth et al., 2017; Sun

et al., 2015). Because modeled  $\text{NH}_3$  neutralized modeled nitric acid and sulfate, a sensitivity run involving increased  $\text{NH}_3$  emissions does not significantly increase 24-h modeled ammonium nitrate concentrations.

Figs. 8 and 9 show the daytime vertical profiles of trace species on Jan 20 at Fresno and Porterville, respectively. Aircraft measurements at Fresno were made repeatedly at local hours 9, 12, and 14. Because mixing layer height was lower early in the morning, here, the vertical



profiles for Fresno were the average of measurements made at hours 12 and 14. Measurement at Porterville were made at hours 8, 10, and 13, and the average of hours 10 and 13 were shown here. Fresno is the largest city in the SJV with a half million population and Porterville is a small rural city with only approximately 50,000 population. Fresno has higher  $\text{NO}$ ,  $\text{NO}_2$ , and  $\text{NO}_y$  concentrations than Porterville, reflecting more  $\text{NO}_x$  emissions at Fresno. Porterville has higher  $\text{NH}_3$  concentrations because it is closer to dairy sources than Fresno, which can be seen in the daily emissions map for  $\text{NO}_x$  and  $\text{NH}_3$  on Jan 20 (Figs. S15 and S16). On this particularly day, Porterville had higher observed  $\text{HNO}_3$  and nitrate concentrations than Fresno, which reflects the regional formation and distribution of  $\text{HNO}_3$  and nitrate in the SJV (Chow et al., 2006; Lurmann et al., 2006; Watson and Chow, 2002). Spatial distributions of model predicted 24-h average nitrate concentrations are shown in Fig. S17 for Jan 20. As shown in Kelly et al. (2018), daytime  $\text{HNO}_3$  formation is favored at urban areas such as Fresno and Bakersfield and nighttime  $\text{HNO}_3$  formation is more prevalent in less urban locations such as the Porterville-Visalia region. At Fresno, the modeled total  $\text{HNO}_3$  concentration is close to the observed total  $\text{HNO}_3$  concentration, while the particulate nitrate concentration was underestimated. A close examination indicated a large fraction of  $\text{HNO}_3$  was in the gas phase in the model, which led to overall under prediction of nitrate concentration (further discussed in the diurnal cycle of ammonium nitrate section). Overall, for all pollutants including VOC species, model performance at those two locations was similar to the SJV average shown in Fig. 7.

#### Diurnal cycle of ammonium nitrate

Ammonium nitrate is the major  $\text{PM}_{2.5}$  component in the SJV and nitric acid is the limiting precursor for ammonium nitrate formation in the SJV. A key pathway for ammonium nitrate formation in the SJV is the nocturnal nitric acid formation in the residual layer followed by the mixing down of nitric acid to the surface next morning. Nitric acid then combines with ammonia to form ammonium nitrate and leads to a morning ammonium nitrate peak (Prabhakar et al., 2017; Watson and Chow, 2002). The other pathway is the daytime oxidation of  $\text{NO}_2$  by hydroxyl radical to form nitric acid (Pusede et al., 2016). During DISCOVER-AQ, an aerosol mass spectrometer (AMS) was deployed at Fresno to measure highly time resolved  $\text{PM}_{1.0}$  (particulate matter with aerodynamic diameter less than  $1.0 \mu\text{m}$ ) non-refractory chemical components (Young et al., 2016). Here, the modeled diurnal cycle of nitrate

and ammonium was compared to the average observations from AMS from January 16 through February 10, 2013. Although AMS measured  $\text{PM}_{1.0}$  species,  $\text{PM}_{1.0}$  species accounted for the majority of  $\text{PM}_{2.5}$  mass (Parworth et al., 2017) and therefore modeled  $\text{PM}_{2.5}$  nitrate and ammonium are used. Fig. 10 shows that the model reproduced the morning increase of ammonium nitrate, capturing the chemistry and dynamics of the nocturnal nitric acid formation pathway. From noon to afternoon, modeled nitrate and ammonium decreased more significantly than observations, which could be due to the internal assumption regarding aerosol states (i.e., metastable versus stable) in CMAQ's aerosol thermodynamic model that governs the gas-particle partitioning of ammonium nitrate (Kelly et al., 2018), as well as an under prediction of ammonia mixing ratios at Fresno during the day.

#### $\text{NO}_2$ column concentrations

Table 2 shows the comparison between observed and modeled daytime  $\text{NO}_2$  column concentrations using measurements from ground-based Pandora systems (Herman et al., 2009) at 12 sites in the SJV. During DISCOVER-AQ, a total of 14 measurements were made at 12 sites in the SJV, including two co-located measurements at Fresno and Porterville, respectively. Observed column  $\text{NO}_2$  concentrations were highest in Fresno and Bakersfield. On average, model predictions were very close to observation at Fresno (i.e., approximately 5% difference), while the model over-predicted observed  $\text{NO}_2$  column concentrations at Bakersfield by 15%. Model predictions and observations were within 40% in all locations except at Shafter and Tranquility. The model under-predicted  $\text{NO}_2$  column concentrations by approximately 50% at those two locations. Shafter is a city located upwind of Bakersfield. Ground based  $\text{NO}_2$  mixing ratios were also measured at Shafter and the model showed a similar level of under prediction. Tranquility is a rural city (see Fig. 1) located away from major mobile source emissions along highway 99. Overall, modeled  $\text{NO}_2$  column concentrations matched well with observations at urban locations such as Fresno and Bakersfield, while under prediction is evident in the more rural sites. A recent paper by Almaraz et al. (2018) suggested that cropland  $\text{NO}_x$  emissions can be comparable to mobile source  $\text{NO}_x$  emissions in the SJV. Given that  $\text{NO}_2$  column concentrations are under predicted by the model at more rural sites, it is possible that this source of  $\text{NO}_x$  emissions needs to be examined in addition to other potential reasons (e.g., spatial allocation of existing emissions, inadequate transport in the model). However, given

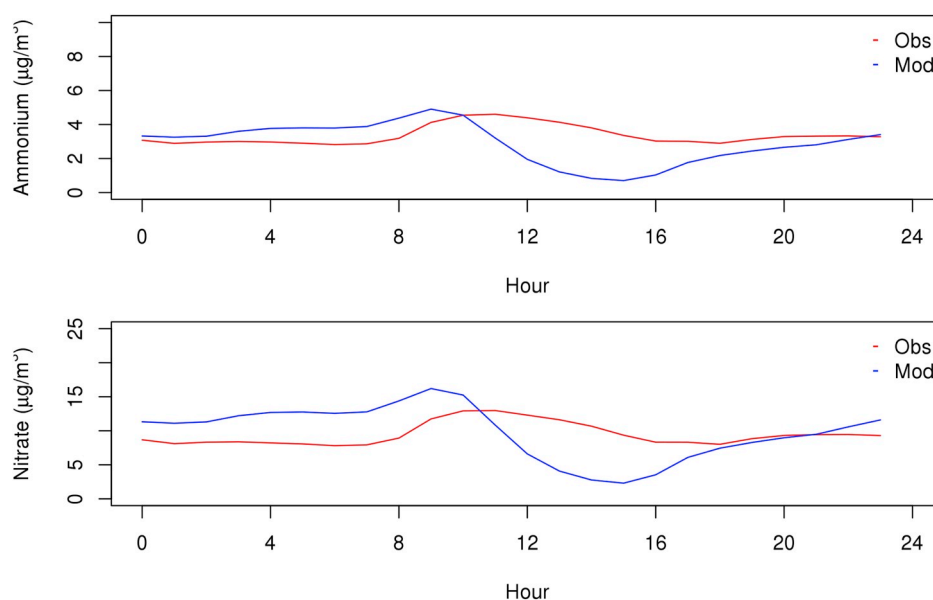


Fig. 10. Average observed and modeled diurnal cycles of ammonium and nitrate from Jan 16- Feb 10.

**Table 2**Model performance statistics for NO<sub>2</sub> column concentrations based on Pandora measurements.

Site	Mean Obs. (x1.0e15 molecules/cm <sup>2</sup> )	Mean Mod. (x1.0e15 molecules/cm <sup>2</sup> )	Mean Bias (x1.0e15 molecules/cm <sup>2</sup> )	Mean Error (x1.0e15 molecules/cm <sup>2</sup> )	MFB (%)	MFE (%)
Arvin	7.5	9.0	1.5	1.5	19	19
Bakersfield	9.7	11.3	1.6	3.3	19	33
Corcoran	5.9	4.3	-1.6	1.6	-32	32
Fresno	11.8	11.4	-0.4	2.0	-1	18
Fresno (2)	12.0	11.2	-0.8	2.0	-5	17
Hanford	5.8	5.2	-0.6	0.7	-11	13
Huron	4.7	3.1	-1.6	1.8	-44	48
Madera	6.2	6.1	-0.1	0.9	0	15
Parlier	8.0	7.0	-1.0	1.5	-15	20
Porterville	7.0	4.2	-2.8	2.8	-51	51
Porterville (2)	6.9	4.4	-2.5	2.5	-45	45
Shafter	7.5	3.6	-4.0	4.0	-73	73
Tranquility	6.3	2.5	-3.8	3.8	-86	86
Visalia	7.1	6.1	-1.1	1.1	-16	17

that NO<sub>2</sub> column concentrations at the more rural sites are typically only approximately 50% of those at Fresno and Bakersfield and the model can capture the NO<sub>2</sub> column concentrations at Fresno & Bakersfield, it is unlikely that NO<sub>x</sub> emissions from croplands are comparable to mobile sources. Fig. S18 also shows the average diurnal profiles of NO<sub>2</sub> column concentrations at Fresno and Porterville. At Fresno, observed NO<sub>2</sub> column concentrations peaked in the afternoon while modeled concentrations decreased in the afternoon. At Porterville, observed and modeled NO<sub>2</sub> column concentrations were both relatively flat, although modeled concentrations were biased low.

## Conclusions

The WRF/CMAQ modeling system was used to simulate air quality during the DISCOVER-AQ field campaign in the SJV during January–February 2013. Model performance for both meteorological parameters and chemical species was evaluated based on ground-based as well as aircraft-based measurements. The unique ambient datasets provided by DISCOVER-AQ enabled more detailed evaluation of the modeling system, particularly with regard to PM<sub>2.5</sub> precursors and vertical pollutant distributions, which were rarely available since the CRPAQS study. Overall model performance is comparable to previous studies in the region, even though the SJV was under prolonged drought conditions and significantly reduced emissions levels compared to the CRPAQS study.

Observed PM<sub>2.5</sub> concentrations started to accumulate from January 10 and peaked on January 22–23 throughout the SJV. The model was able to capture gradual accumulation of PM<sub>2.5</sub> from January 10, but peaked on January 21 (1–2 days earlier than observed). This slight difference in observed and modeled peak days likely indicated that further improvement in meteorological fields was needed. After January 28, observed PM<sub>2.5</sub> concentrations started to increase again and peaked on February 2–4, particularly in the southern portion of the SJV. Modeled PM<sub>2.5</sub> concentrations also showed similar evolution. Overall, the variations of daily PM<sub>2.5</sub> concentrations from January 10 to February 10 were captured by the model reasonably well. On average, peak PM<sub>2.5</sub> concentrations were somewhat under predicted by the model. At individual sites, the model under-predicted peak concentrations at Bakersfield, likely because Bakersfield is located in the southern portion of the valley and is subject to more influence from the transport and mixing within the SJV. In terms of PM<sub>2.5</sub> composition, both observations and model showed that PM<sub>2.5</sub> in the SJV was dominated by ammonium nitrate and OC. Modeled OC was dominated by primary sources with very little contribution from SOA. AMS measurement showed a substantial fraction of oxygenated organic aerosol in Fresno that was suggested to be of secondary nature (Young et al., 2016). However, wintertime SOA formation mechanism and sources are not

clear yet and require further study.

Comparison to aircraft measurements made on January 20 showed that there was general agreement in the observed and modeled vertical distributions of NO, NO<sub>2</sub>, HNO<sub>3</sub>, and NO<sub>y</sub> concentrations. The model produced an adequate amount of HNO<sub>3</sub>, which is the limiting precursor for ammonium nitrate in the valley. It, also, under-predicted mixing ratios of formaldehyde and acetaldehyde. These species are primarily secondary and improved treatment of chemistry and more explicit precursor emissions are likely needed to achieve better agreement. Both observations and the model showed that O<sub>3</sub> mixing ratios were smaller in the mixing layer than in the free troposphere due to titration by fresh NO<sub>x</sub> emissions at the surface. The model showed excess NH<sub>3</sub> in the SJV and that the formation of ammonium nitrate was limited by the availability of HNO<sub>3</sub>, even though it under predicted NH<sub>3</sub> mixing ratios. Comparison of the ammonium nitrate diurnal profile revealed that the observed morning increase of ammonium nitrate due to downward mixing of nocturnal HNO<sub>3</sub> formed in the residual layer was also evident in the model. In addition, comparison of column NO<sub>2</sub> measurements showed that modeled column concentrations agreed with measured concentrations at urban locations but were under predicted at more rural locations.

This paper demonstrated that the WRF/CMAQ modeling system was able to capture elevated PM<sub>2.5</sub> episodes in the SJV during the DISCOVER-AQ period when SJV was in severe drought conditions. Therefore, the current WRF/CMAQ modeling system is suitable for supporting the SJV PM<sub>2.5</sub> SIP development. Future improvement in meteorological modeling in simulating stagnant conditions is still needed given that there is still some difference between observed and model predicted timing of peak concentrations. In addition, there is also a need for constraining CMAQ model predictions of daytime versus nighttime nitric acid formation rates. This will require measurements or derivation of daytime and nighttime radical concentrations (e.g., hydroxyl and nitrate radicals) in the SJV. AMS measurements during DISCOVER-AQ suggested a large fraction of oxygenated organic aerosol that was not predicted by the CMAQ model. This requires further improvement in model treatment of additional VOC precursors and atmospheric processing of organic aerosols. Finally, given the low boundary layer height during the stagnant conditions, model prediction of PM<sub>2.5</sub> concentrations can be very sensitive to the amount of emissions and their spatial and temporal allocations. Therefore, better characterization of emissions is also warranted, particularly for sources that are highly dependent on meteorological conditions.

## Disclaimer

This paper has been reviewed by the staff of the California Air Resources Board and has been approved for publication. Approval does not

signify that the contents necessarily reflect the views and policies of the California Air Resources Board, nor does mention of trade names or commercial products constitute endorsement or recommendation for use.

### Declaration of competing interest

The authors declare that they have no known competing financial interests or personal relationships that could have appeared to influence the work reported in this paper.

### CRediT authorship contribution statement

**Jianjun Chen:** Conceptualization, Methodology, Software, Validation, Formal analysis, Writing - original draft, Writing - review & editing. **Dazhong Yin:** Methodology, Software, Validation, Formal analysis. **Zhan Zhao:** Methodology, Software, Validation, Formal analysis. **Ajith P. Kaduwela:** Conceptualization, Methodology, Writing - original draft, Writing - review & editing, Supervision. **Jeremy C. Avice:** Conceptualization, Methodology, Writing - original draft, Writing - review & editing, Supervision. **John A. DaMassa:** Conceptualization, Methodology, Writing - original draft, Writing - review & editing, Supervision. **Andreas Beyersdorf:** Investigation. **Sharon Burton:** Investigation. **Richard Ferrare:** Investigation. **Jay R. Herman:** Investigation. **Hwajin Kim:** Investigation. **Andy Neuman:** Investigation. **John B. Nowak:** Investigation. **Caroline Parworth:** Investigation. **Amy Jo Scarino:** Investigation. **Armin Wisthaler:** Investigation. **Dominique E. Young:** Investigation. **Qi Zhang:** Investigation.

### Acknowledgments

We thank Professor Ronald C. Cohen at the University of California, Berkeley for providing nitric acid observations aboard NASA P3B, Andrew J. Weinheimer and Denise D. Montzka at the National Center for Atmospheric Research for providing NO, NO<sub>2</sub>, NO<sub>y</sub>, and O<sub>3</sub> observations aboard NASA P3B, and Alan Fried and James Walega of the University of Colorado, Boulder for providing formaldehyde measurement observations aboard NASA P3B. PTR-ToF-MS measurements aboard the NASA P3B during DISCOVER-AQ were supported by the Austrian Federal Ministry for Transport, Innovation and Technology (bmvit) through the Austrian Space Applications Program (ASAP) of the Austrian Research Promotion Agency (FFG). The PTR-MS instrument team (T. Mikoviny, M. Müller) is acknowledged for their support with field work and data processing.

### Appendix A. Supplementary data

Supplementary data to this article can be found online at <https://doi.org/10.1016/j.aeaoa.2020.100067>.

### References

- Almaraz, M., Bai, E., Wang, C., Trousdell, J., Conley, S., Faloona, I., Houlton, B.Z., 2018. Agriculture is a major source of NO<sub>x</sub> pollution in California. *Science Advances* 4. <https://doi.org/10.1126/sciadv.aao3477>.
- American Lung Association, 2018. State of the air. <https://www.lung.org/asset/s/documents/healthy-air/state-of-the-air/sota-2018-full.pdf>.
- Bao, J.W., Michelson, S.A., Persson, P.O.G., Djalalova, I.V., Wilczak, J.M., 2008. Observed and WRF-simulated low-level winds in a high-ozone episode during the Central California Ozone Study. *Journal of Applied Meteorology and Climatology* 47, 2372–2394.
- Boylan, J.W., Russell, A.G., 2006. PM and light extinction model performance metrics, goals, and criteria for three-dimensional air quality models. *Atmos. Environ.* 40, 4946–4959.
- Brooks, I.M., 2003. Finding boundary layer top: application of wavelet covariance transformation to Lidar backscatter profiles. *J. Atmos. Ocean. Technol.* 20, 1092–1105.
- Brown, S.G., Roberts, P.T., McCarthy, M.C., Lurmann, F.W., Hyslop, N.P., 2006. Wintertime vertical variations in particulate matter (PM) and precursor concentrations in the San Joaquin Valley during the California Regional coarse PM/fine PM Air Quality Study. *J. Air Waste Manag. Assoc.* 56, 1267–1277, 2006.
- Cai, C., et al., 2016. Simulating reactive nitrogen, carbon monoxide, and ozone in California during ARCTAS-CARB 2008 with high wildfire activity. *Atmos. Environ.* 128, 28–44.
- Carb, 2012. Photochemical Modeling for the 24-hour PM<sub>2.5</sub> State Implementation Plan in the San Joaquin Valley, Prepared by California Air Resources Board for the United States Environmental Protection Agency Region IX.
- Carter, W.P.L., 2010. Development of the SAPRC-07 Chemical Mechanism and Updated Ozone Reactivity Scales, Report to the California Air Resources Board by. The University of California, Riverside.
- Chen, J., Lu, J., Avice, J.C., DaMassa, J.A., Kleeman, M.J., Kaduwela, A.P., 2014. Seasonal modeling of PM<sub>2.5</sub> in California's San Joaquin Valley. *Atmos. Environ.* 92, 182–190.
- Chen, J., Ying, Q., Kleeman, M.J., 2009. Source apportionment of visual impairment during the California regional PM<sub>10</sub>/PM<sub>2.5</sub> air quality study. *Atmos. Environ.* 43, 6136–6144.
- Chen, J., Ying, Q., Kleeman, M.J., 2010. Source apportionment of wintertime secondary organic aerosol during the California regional PM<sub>10</sub>/PM<sub>2.5</sub> air quality study. *Atmos. Environ.* 44, 1331–1340.
- Chow, J.C., Chen, L.W.A., Watson, J.G., Lowenthal, D.H., Magliano, K.A., Turkiewicz, K., Lehman, D.E., 2006. PM<sub>2.5</sub> chemical composition and spatiotemporal variability during the California Regional PM<sub>10</sub>/PM<sub>2.5</sub> Air Quality Study (CRPAQS). *J. Geophys. Res.* 111, D10S04. <https://doi.org/10.1029/2005JD006457>.
- Davis, J.M., Bhawe, P.V., Foley, K.M., 2008. Parameterization of N<sub>2</sub>O<sub>5</sub> reaction probabilities on the surface of particles containing ammonium, sulfate, and nitrate. *Atmos. Chem. Phys.* 8, 5295–5311.
- Eder, B., Yu, S., 2006. A performance evaluation of the 2004 release of Models-3 CMAQ. *Atmos. Environ.* 40, 4811–4824.
- Emmons, L.K., et al., 2010. Description and evaluation of the model for ozone and related chemical Tracers, version 4 (MOZART-4). *Geosci. Model Dev. (GMD)* 3, 43–67.
- Ge, X., Setyan, A., Sun, Y., Zhang, Q., 2012a. Primary and secondary organic aerosols in Fresno, California during wintertime: results from high resolution aerosol mass spectrometry. *Journal of Geophysical Research-Atmospheres* D19301. <https://doi.org/10.1029/2012JD018026>.
- Ge, X., Zhang, Q., Sun, Y., Ruehl, C.R., Setyan, A., 2012b. Effect of aqueous-phase processing on aerosol chemistry and size distribution in Fresno, California, during wintertime. *Environ. Chem.* 9, 221–235.
- Held, T., Ying, Q., Kaduwela, A., Kleeman, M.J., 2004. Modeling particulate matter in the San Joaquin Valley with a source-oriented externally mixed three-dimensional photochemical grid model. *Atmos. Environ.* 38, 3689–3711.
- Herman, J., Cede, A., Spinei, E., Mount, G., Tzortziou, M., Abuhassan, N., 2009. NO<sub>2</sub> column amounts from ground-based Pandora and MFDAS spectrometers using the direct-sun DOAS technique: intercomparisons and application to OMI validation. *J. Geophys. Res.* 114, D13307. <https://doi.org/10.1029/2009JD011848>.
- Hu, J., Ying, Q., Chen, J., Mahmud, A., Zhao, Z., Chen, S.H., Kleeman, M.J., 2010. Particulate air quality model predictions using prognostic vs. diagnostic meteorology in central California. *Atmos. Environ.* 44, 215–226.
- Hu, J., Zhang, H., Chen, S., Ying, Q., Wiedinmyer, C., Vandenbergh, F., Kleeman, M.J., 2014a. Identifying PM<sub>2.5</sub> and PM<sub>0.1</sub> sources for epidemiological studies in California. *ES T (Environ. Sci. Technol.)* 48, 4980–4990.
- Hu, J., Zhang, H., Ying, Q., Chen, S.H., Vandenbergh, F., Kleeman, M.J., 2014b. Long-term particulate matter modeling for health effects studies in California – Part 1: model performance on temporal and spatial variations. *Atmos. Chem. Phys.* 15, 3445–3461.
- Kelly, J.T., et al., 2014. Fine-scale simulation of ammonium and nitrate over the south coast air basin and San Joaquin Valley of California during CalNex-2010. *Journal of Geophysical Research - Atmosphere* 119, 3600–3614. <https://doi.org/10.1002/2013JD021290>.
- Kelly, J.T., et al., 2018. Modeling NH<sub>4</sub>NO<sub>3</sub> over the San Joaquin Valley during the 2013 DISCOVER-AQ campaign. *Journal of Geophysical Research - Atmosphere* 123, 4727–4745. <https://doi.org/10.1029/2018JD028290>.
- Kleeman, M.J., Ying, Q., Kaduwela, A., 2005. Control strategies for the reduction of airborne particulate nitrate in California's San Joaquin Valley. *Atmos. Environ.* 39, 5325–5341.
- Livingstone, P.L., et al., 2009. Simulating PM concentration during a winter episode in a subtropical valley: sensitivity simulations and evaluation methods. *Atmos. Environ.* 43, 5971–5977.
- Lueken, D.J., Hutzell, W.T., Strum, M.L., Pouliot, G.A., 2012. Regional sources of atmospheric formaldehyde and acetaldehyde, and implications for atmospheric modeling. *Atmos. Environ.* 47, 477–490.
- Lurmann, F.W., Brown, S.G., McCarthy, M.C., Roberts, P.T., 2006. Processes influencing secondary aerosol formation in the San Joaquin Valley during winter. *J. Air Waste Manag. Assoc.* 56, 1679–1693.
- MacDonald, C.P., McCarthy, M.C., Dye, T.S., Wheeler, N.J.M., Hafner, H.R., Roberts, P.T., 2006. Transport and dispersion during wintertime particulate matter episodes in the San Joaquin Valley, California. *J. Air Waste Manag. Assoc.* 56, 961–976.
- Mahmud, A., Hixson, M., Hu, J., Zhao, Z., Chen, S.H., Kleeman, M.J., 2010. Climate impact on airborne particulate matter concentrations in California using seven year analysis periods. *Atmos. Chem. Phys.* 10, 11097–11114.
- Markovic, M.Z., VandenBoer, T.C., Baker, K.R., Kelly, J.T., Murphy, J.G., 2014. Measurements and modeling of the inorganic chemical composition of fine particulate matter and associated precursor gases in California's San Joaquin Valley during CalNex 2010. *Journal of Geophysical Research - Atmosphere* 119, 6853–6866. <https://doi.org/10.1002/2013JD021408>.

- Misztal, P.K., Avise, J.C., Karl, T., Scott, K., Jonsson, H.H., Guenther, A.B., Goldstein, A.H., 2016. Evaluation of regional isoprene emission factors and modeled fluxes in California. *Atmos. Chem. Phys.* 16, 9611–9628. <https://doi.org/10.5194/acp-16-9611-2016>.
- Orozco, D., et al., 2016. Hygroscopicity measurements of aerosol particles in the San Joaquin Valley, CA, Baltimore, MD, and Golden, CO. *Journal of Geophysical Research-Atmospheres* 121, 7344–7359. <https://doi.org/10.1002/2015JD023971>.
- Otte, T.L., Pleim, J.E., 2010. The Meteorology-Chemistry Interface Processor (MCIP) for the CMAQ Modeling System: Updates through MCIPv3.4.1, vol. 3. Geoscientific Model Development, pp. 243–256.
- Parworth, C.L., Young, D.E., Kim, H., Zhang, X., Cappa, C.D., Collier, S., Zhang, Q., 2017. Wintertime water-soluble aerosol composition and particle water content in Fresno, California. *Journal of Geophysical Research – Atmosphere* 122, 3155–3170. <https://doi.org/10.1002/2016JD026173>.
- Prabhakar, G., et al., 2017. Observational assessment of the role of nocturnal residual-layer chemistry in determining daytime surface particulate nitrate concentrations. *Atmos. Chem. Phys.* 17, 14747–14770.
- Pollack, I.B., Ryerson, T.B., Trainer, M., Neuman, J.A., Roberts, J.M., Parrish, D.D., 2013. Trends in ozone, its precursors, and related secondary oxidation products in Los Angeles, California: a synthesis of measurements from 1960 to 2010. *Geophys. Res. Lett.* 118, 5893–5911.
- Pun, B.K., Balmori, R.T.F., Seigneur, C., 2009. Modeling wintertime particulate matter formation in central California. *Atmos. Environ.* 43, 402–409.
- Pusede, S.E., Cohen, R.C., 2012. On the observed response of ozone to NO<sub>x</sub> and VOC reactivity reductions in San Joaquin Valley California 1995 – present. *Atmos. Chem. Phys.* 12, 8323–8339.
- Pusede, S.E., et al., 2016. On the effectiveness of nitrogen oxide reductions as a control over ammonium nitrate aerosol. *Atmos. Chem. Phys.* 16, 2575–2596.
- Russell, A.R., Valin, L.C., Busceta, E.J., Wenig, M.O., Cohen, R.C., 2010. Space-based constraints on spatial and temporal patterns of NO<sub>x</sub> emissions in California, 2005–2008. *Environ. Sci. Technol.* 44, 3608–3615.
- Scarino, A.J., et al., 2014. Comparison of mixed layer heights from airborne high spectral resolution lidar, ground-based measurements, and the WRF-chem model during CalNex and CARES. *Atmos. Chem. Phys.* 14, 5547–5560.
- SJVAPCD, 2016. Proposed 2016 Plan for the 2008 8-Hour Ozone Standard, Appendix J Modeling Emission Inventory. [http://www.valleyair.org/Workshops/public\\_worksh\\_ops\\_idx.htm#06-16-16-OzoneStandard](http://www.valleyair.org/Workshops/public_worksh_ops_idx.htm#06-16-16-OzoneStandard).
- Simon, H., Baker, K.R., Philips, S., 2012. Compilation and interpretation of photochemical model performance statistics published between 2006 and 2012. *Atmos. Environ.* 61, 124–139.
- Solomon, P.A., Magliano, K.L., 1999. The 1995-Integrated Monitoring Study (IMS95) of the California Regional PM<sub>10</sub>/PM<sub>2.5</sub> air quality study (CRPAQS): study overview. *Atmos. Environ.* 33, 4747–4756.
- Sun, K., et al., 2015. Validation of TES ammonia observations at the single pixel scale in the San Joaquin Valley during DISCOVER-AQ. *Journal of Geophysical Research-Atmosphere* 120, 5140–5154. <https://doi.org/10.1002/2014JD022846>.
- Turkiewicz, K., Magliano, K., Najita, T., 2006. Comparison of two winter air quality episodes during the California regional particulate air quality study. *J. Air Waste Manag. Assoc.* 56, 467–473.
- U.S.Epa, 2007. Guidance on the Use of Models and Other Analyses for Demonstrating Attainment of Air Quality Goals for Ozone, PM<sub>2.5</sub>, and Regional Haze. U.S. Environmental Protection Agency. Research Triangle Park, North Carolina, available at: <https://www3.epa.gov/scram001/guidance/guide/final-03-pm-rh-guidance>.
- U.S. Epa, 2018. San Joaquin Valley. <https://www.epa.gov/sanjoaquinvalley>.
- Watson, J.G., Chow, J.C.A., 2002. Wintertime PM<sub>2.5</sub> episode at the Fresno, CA. Supersite, *Atmospheric Environment* 36, 465–475.
- Ying, Q., Lu, J., Allen, P., Livingstone, P., Kaduwela, A., Kleeman, M.J., 2008a. Modeling air quality during the California Regional PM<sub>10</sub>/PM<sub>2.5</sub> Air Quality Study (CRPAQS) using the UCD/CIT source-oriented air quality model – Part I. Base case model results. *Atmos. Environ.* 42, 8954–8966.
- Ying, Q., Lu, J., Kaduwela, A., Kleeman, M.J., 2008b. Modeling air quality during the California regional PM<sub>10</sub>/PM<sub>2.5</sub> air quality study (CPRAQS) using the UCD/CIT source oriented air quality model - Part II. Regional source apportionment of primary airborne particulate matter. *Atmos. Environ.* 42, 8967–8978.
- Ying, Q., Lu, J., Kleeman, M.J., 2009. Modeling air quality during the California Regional PM<sub>10</sub>/PM<sub>2.5</sub> Air Quality Study (CPRAQS) using the UCD/CIT source-oriented air quality model - Part III. Regional source apportionment of secondary and total airborne particulate matter. *Atmos. Environ.* 43, 419–430.
- Young, D.E., Kim, H., Parworth, C., Zhou, S., Zhang, X., Cappa, C.D., Seco, R., Kim, S., Zhang, Q., 2016. Influences of emission sources and meteorology on aerosol chemistry in a polluted urban environment: results from DISCOVER-AQ California. *Atmos. Chem. Phys.* 16, 5427–5451.
- Yu, H., Russell, A., Mulholland, J., Odman, T., Hu, Y., Chang, H., Kumar, N., 2018. Cross-comparison and evaluation of air pollution field estimation methods. *Atmos. Environ.* 179, 49–60.
- Zhang, H., DeNero, S.P., Joe, D.K., Lee, H.H., Chen, S.H., Michalakes, J., Kleeman, M.J., 2014. Development of a source oriented version of the WRF/Chem model and its application to the California regional PM<sub>10</sub>/PM<sub>2.5</sub> air quality study. *Atmos. Chem. Phys.* 14, 485–503.
- Zhang, X., Kim, H., Parworth, C., Zhang, Q., Metcalf, A.R., Cappa, C.D., 2016. Optical properties of wintertime aerosols from residential wood burning in Fresno, CA: results from DISCOVER-AQ 2013. *Environ. Sci. Technol.* 50, 1681–1690.
- Zhang, Y., Liu, P., Liu, X., Pun, B., Seigneur, C., Jacobson, M.Z., Wang, W., 2010. Fine scale modeling of wintertime aerosol mass, number, and size distributions in Central California. *J. Geophys. Res.* 115, D15207. <https://doi.org/10.1029/2009JD012950>.
- Zhao, Z., Chen, S.H., Kleeman, M.J., Tyree, M., Cayan, D., 2011. The impact of climate change on air quality –related meteorological conditions in California. Part I: present time simulation analysis. *J. Clim.* 24, 3344–3361. <https://doi.org/10.1175/2011JCLI3849.1>.



Supplementary:

## **Modeling Air Quality in the San Joaquin Valley of California during the 2013 DISCOVER-AQ Field Campaign**

Jianjun Chen<sup>1</sup>, Dazhong Yin<sup>1</sup>, Zhan Zhao<sup>1</sup>, Ajith P. Kaduwela<sup>1,2</sup>, Jeremy C. Avise<sup>1,3</sup>, John A. DaMassa<sup>1</sup>, Andreas Beyersdorf<sup>4</sup>, Sharon Burton<sup>5</sup>, Richard Ferrare<sup>5</sup>, Jay R. Herman<sup>6</sup>, Hwajin Kim<sup>7</sup>, Andy Neuman<sup>8,9</sup>, John B. Nowak<sup>5</sup>, Caroline Parworth<sup>7</sup>, Amy Jo Scarino<sup>5</sup>, Armin Wisthaler<sup>10,11</sup>, Dominique E. Young<sup>7</sup>, and Qi Zhang<sup>7</sup>

<sup>1</sup> Air Quality Planning and Science Division, California Air Resources Board, Sacramento, CA, USA

<sup>2</sup> Air Quality Research Center, University of California, Davis, CA, USA

<sup>3</sup> Department of Civil and Environmental Engineering, Washington State University, Pullman, WA, USA

<sup>4</sup> Department of Chemistry & Biochemistry, California State University, San Bernardino, CA, USA

<sup>5</sup> NASA Langley Research Center, Hampton, VA, USA

<sup>6</sup> NASA Goddard Space Flight Center, Greenbelt, MD, USA

<sup>7</sup> Department of Environmental Toxicology, University of California, Davis, CA, USA

<sup>8</sup> NOAA Earth System Research Laboratory, Boulder, CO, USA

<sup>9</sup> Cooperative Institute for Research in Environmental Sciences, University of Colorado, Boulder, CO, USA

<sup>10</sup> Institute for Ion Physics and Applied Physics, University of Innsbruck, Innsbruck, Austria

<sup>11</sup> Department of Chemistry, University of Oslo, Oslo, Norway

**Table S1:** Model performance statistics for 24-hour average PM<sub>2.5</sub> concentrations based on surface BAM measurements

Sites	Avg Obs. (µg/m <sup>3</sup> )	Avg Mod. (µg/m <sup>3</sup> )	Mean Bias (µg/m <sup>3</sup> )	Mean Error (µg/m <sup>3</sup> )	MFB (%)	MFE (%)
Bakersfield-Municipal Airport	33.3	24.3	-9.1	14.2	-12	44
Bakersfield-5558 California Avenue	32.0	26.5	-5.5	10.7	-6	34
Fresno-Drummond Street	31.3	26.6	-4.7	9.3	-7	36
Fresno-Garland	29.3	24.7	-4.6	7.5	-15	29
Hanford	27.4	27.2	-0.2	7.4	12	33
Visalia	26.5	28.8	2.3	8.8	17	40
Turlock	26.4	26.4	0.0	7.5	-1	32
Stockton	24.8	22.1	-2.7	6.8	-6	30
Porterville	24.7	23.4	-1.4	6.9	4	30
Clovis	23.4	22.3	-1.1	7.4	0	37
Modesto	21.8	24.6	2.8	7.6	25	44
Madera	20.5	20.4	-0.1	6.5	-1	37
Huron	19.7	11.1	-8.6	8.6	-58	59
Manteca	19.3	23.5	4.2	7.1	26	37
Merced	18.6	22.7	4.1	7.4	22	38
Tranquility	15.0	14.1	-0.8	5.3	-2	40
Tracy	11.7	12.0	0.3	6.5	-10	51
Springville	10.7	8.3	-2.3	4.3	-21	45
Sequoia and Kings Canyon Natl Park	5.6	4.4	-1.2	2.8	-20	58
Lebec	4.3	2.8	-1.5	1.8	-42	53

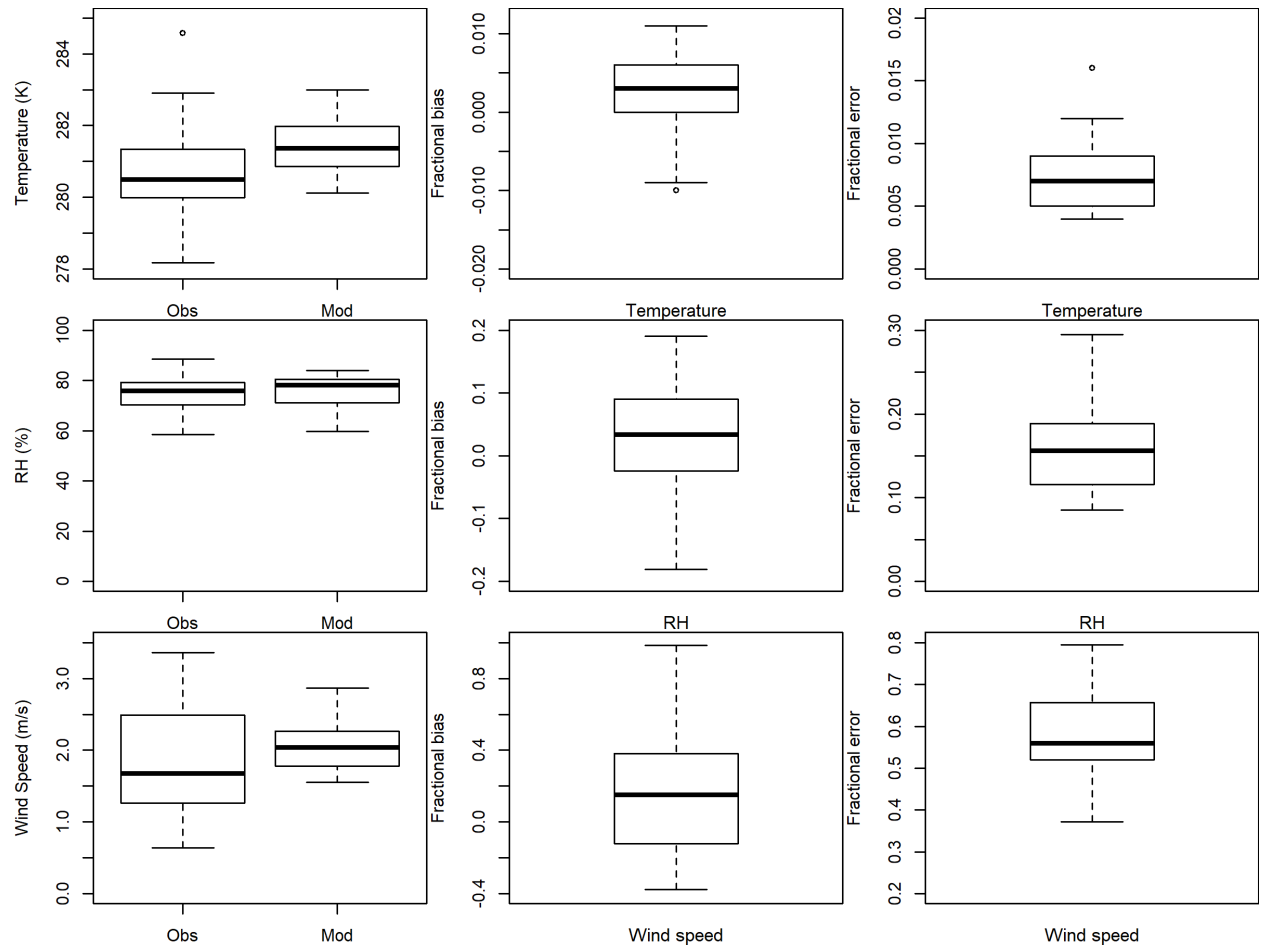


Figure S1: Box plot of mean observations (Obs), mean predictions (Mod), mean fractional bias, and mean fractional errors at all stations in the SJV for surface meteorological parameters.

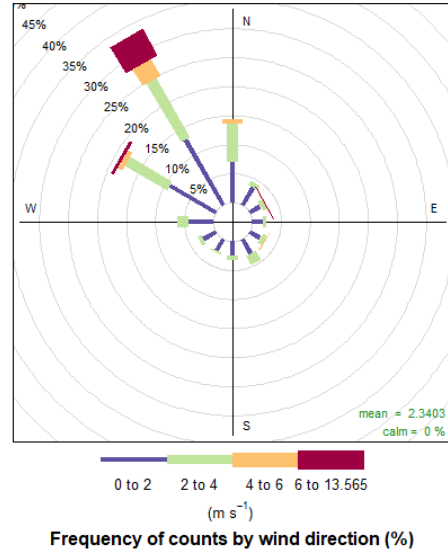
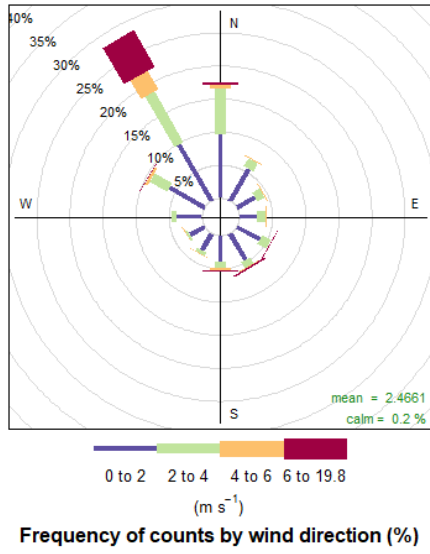


Figure S2: Wind rose comparison between observation (Left) and prediction (Right) for winds below 500 meters at Visalia.

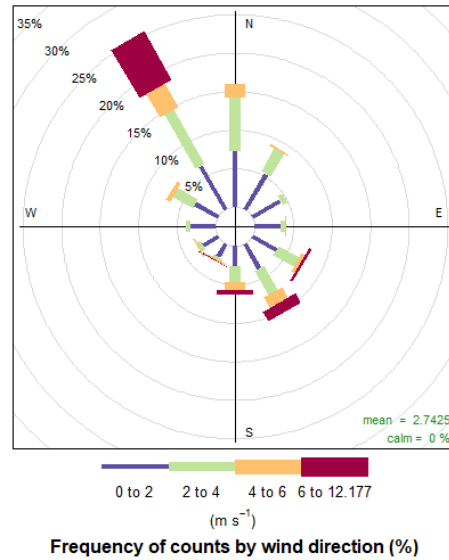
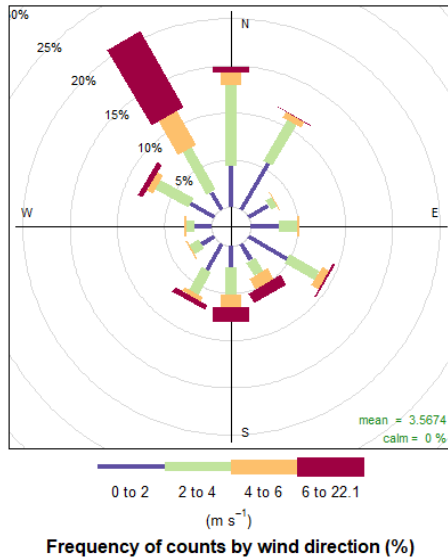


Figure S3: Wind rose comparison between observation (Left) and prediction (Right) for winds between 500 and 1000 meters at Visalia.



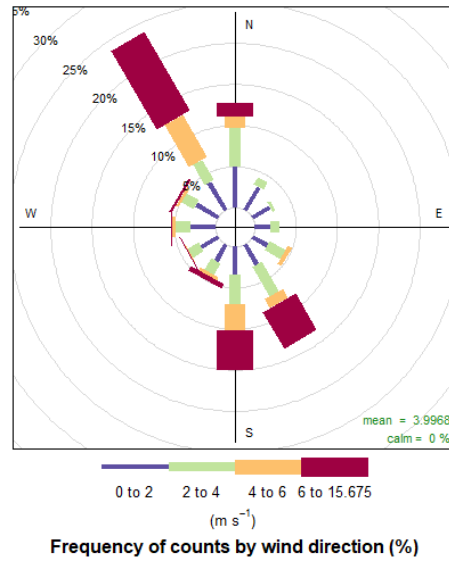
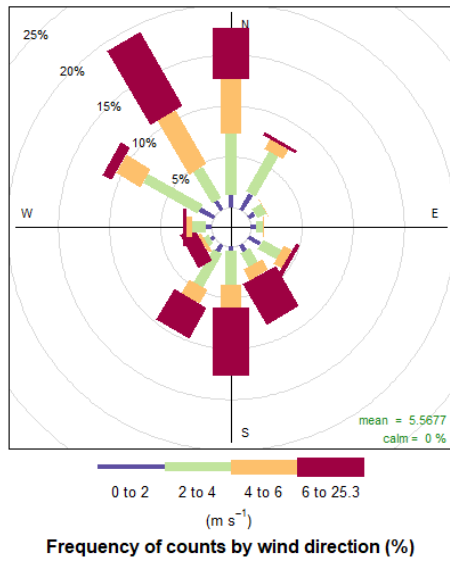


Figure S4: Wind rose comparison between observation (Left) and prediction (Right) for winds between 1000 and 2000 meters at Visalia.

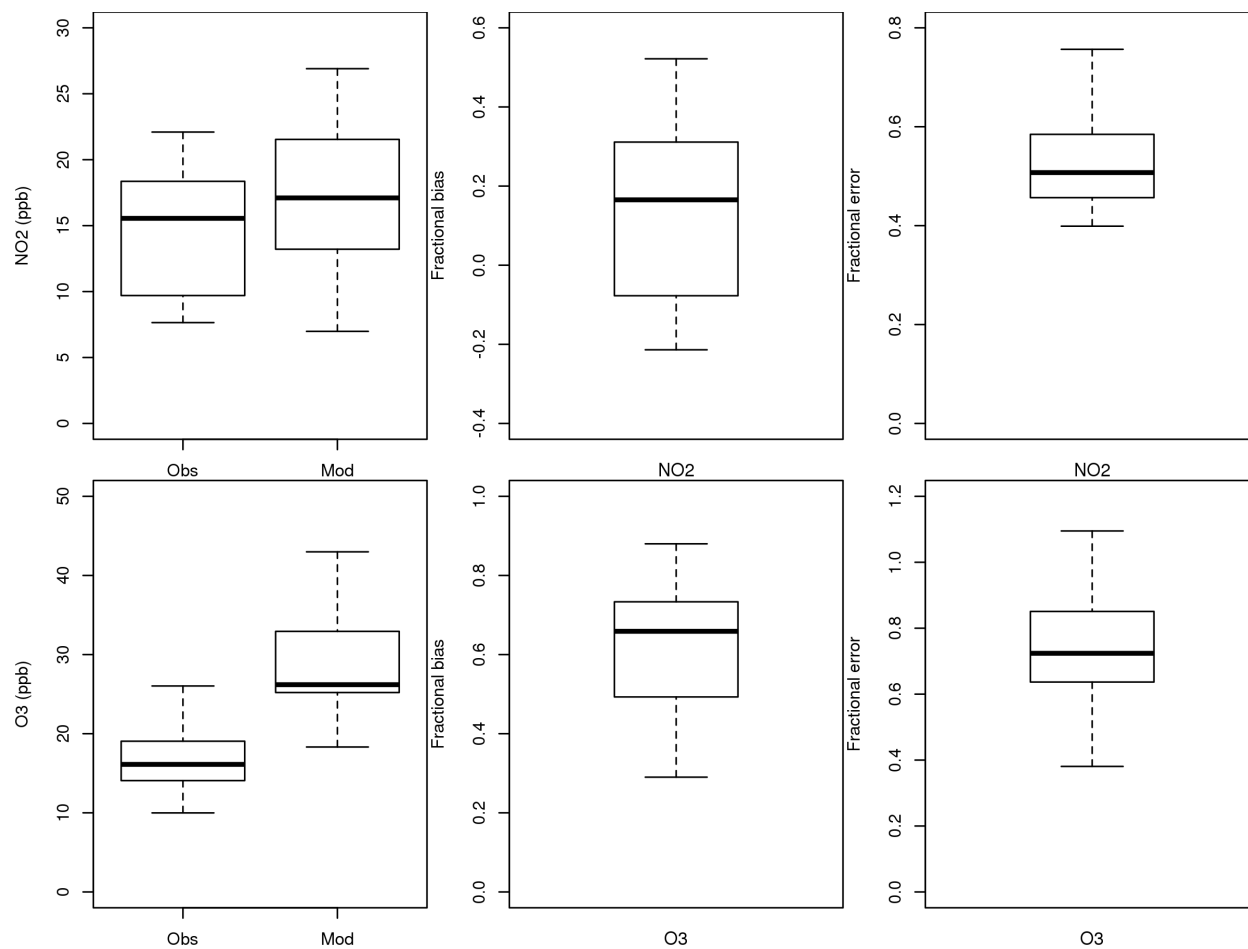
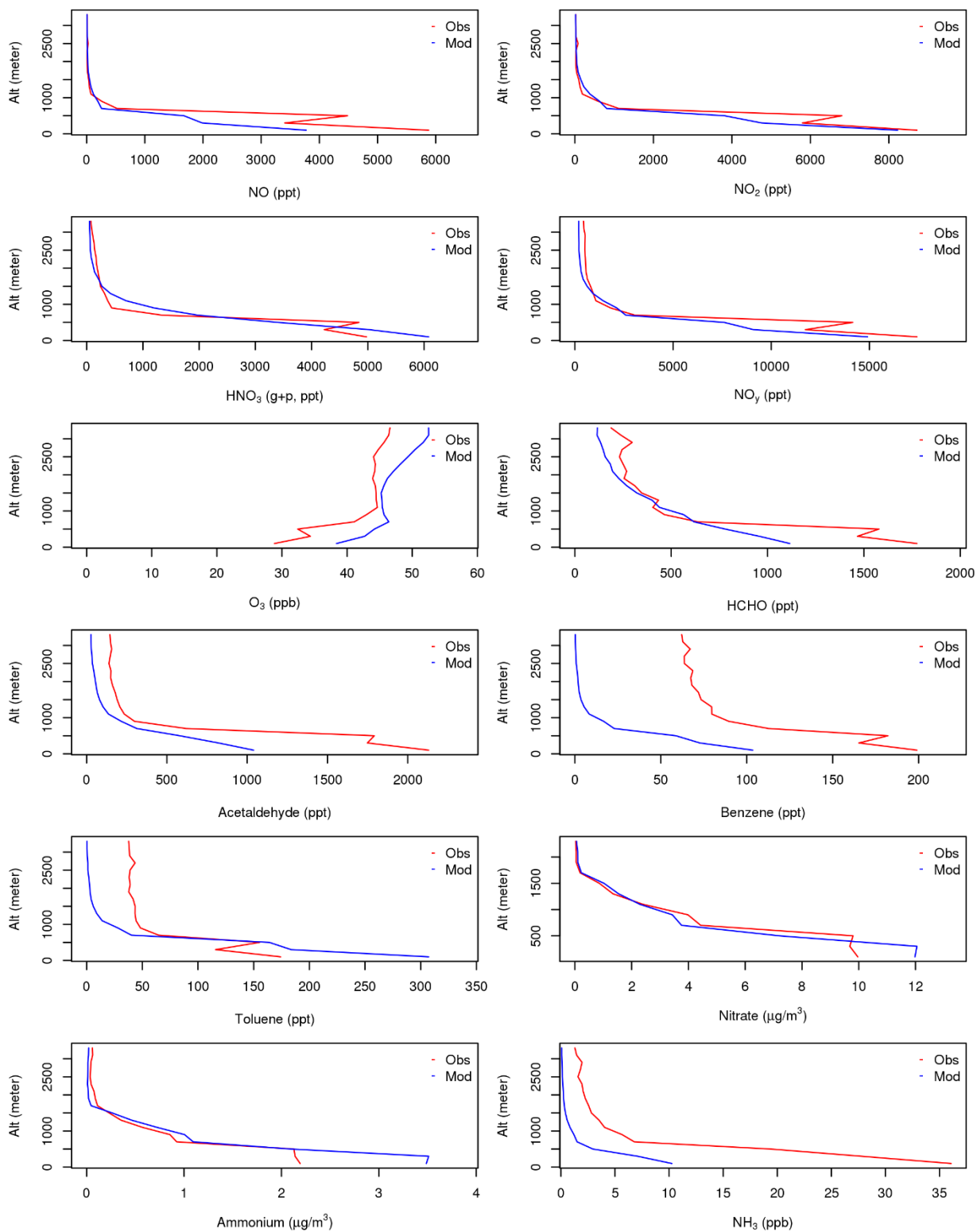


Figure S5: Box plot of mean observations (Obs), mean predictions (Mod), mean fractional bias, and mean fractional errors at surface monitors in the SJV for hourly O<sub>3</sub> and NO<sub>2</sub> mixing ratios.



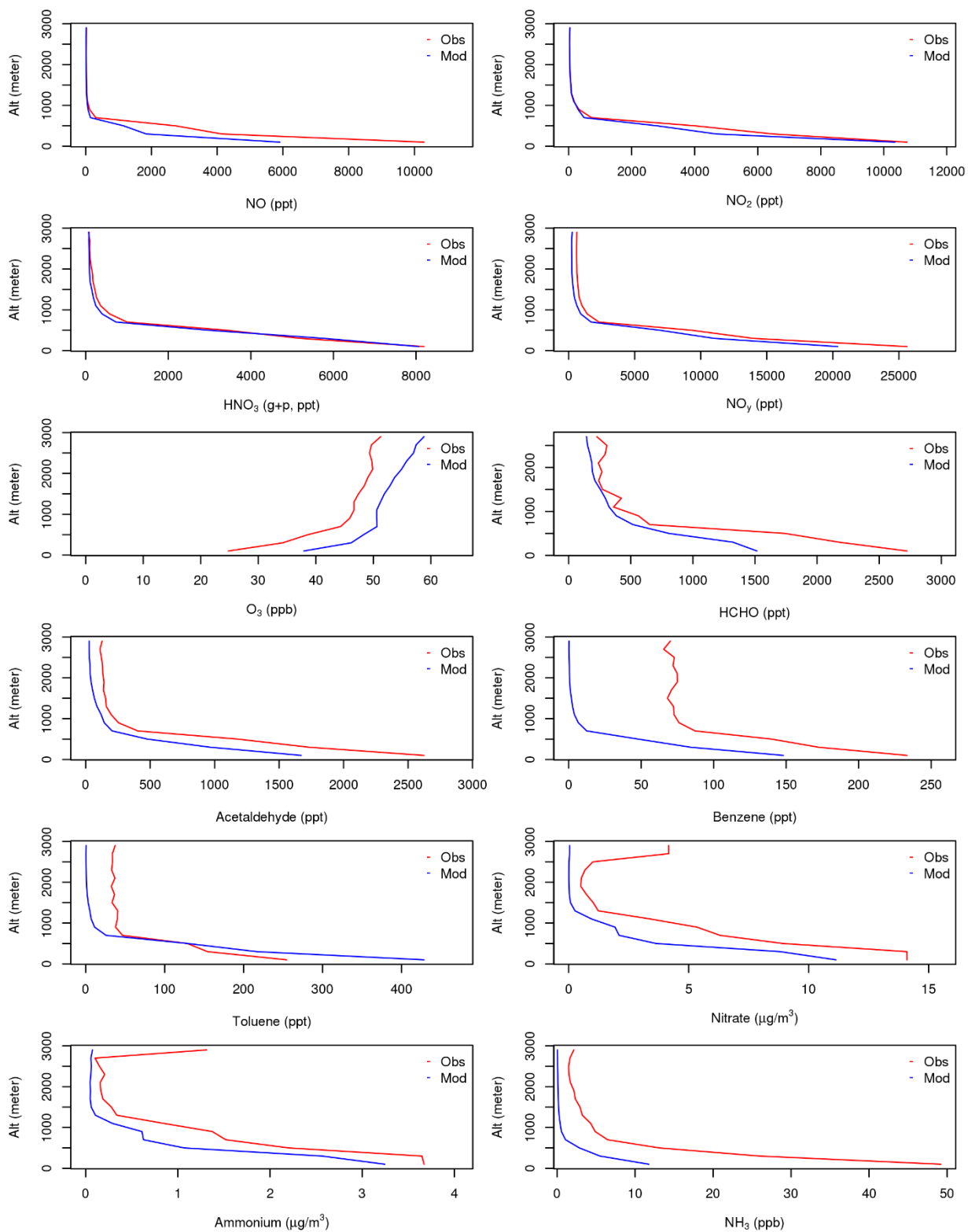
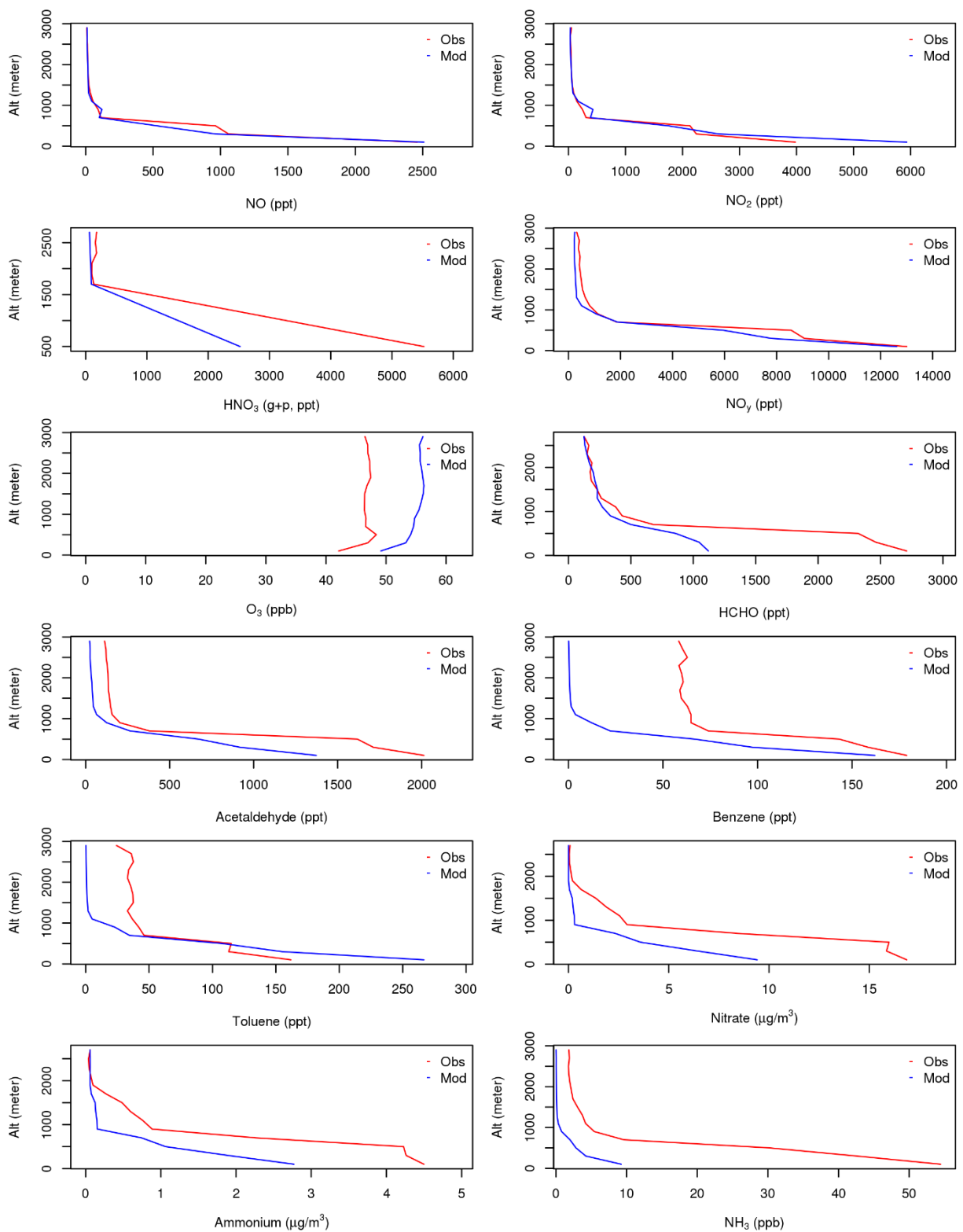
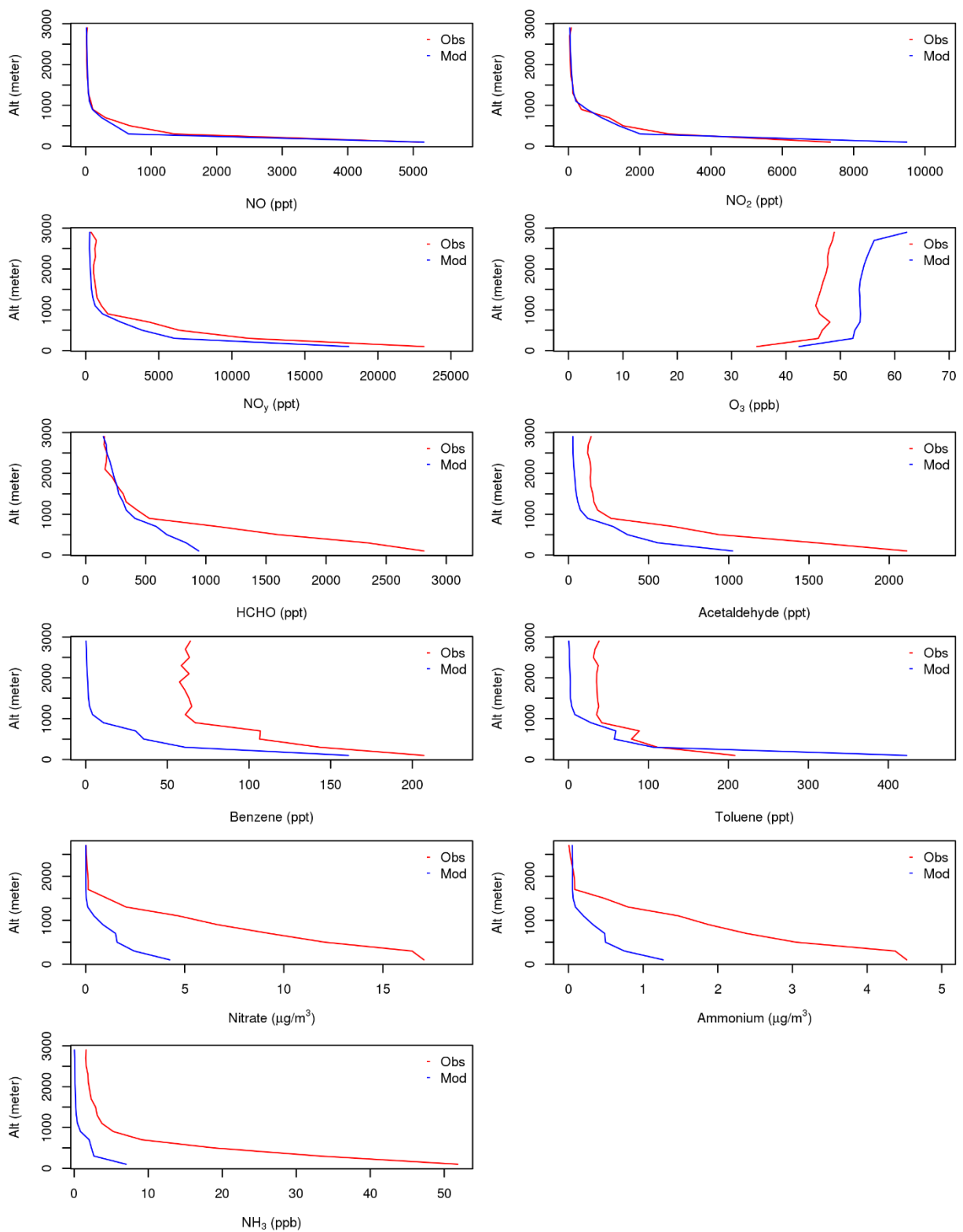
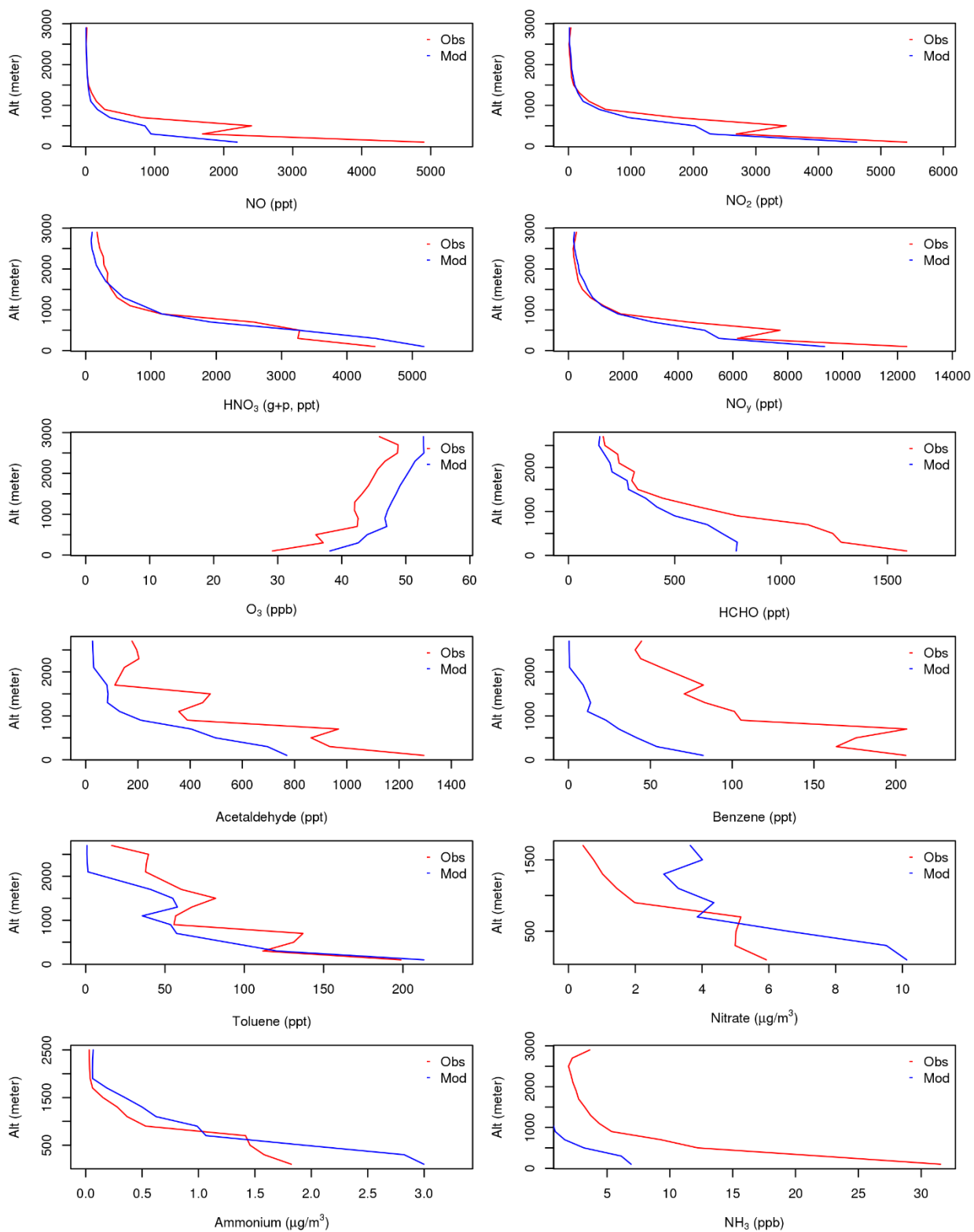


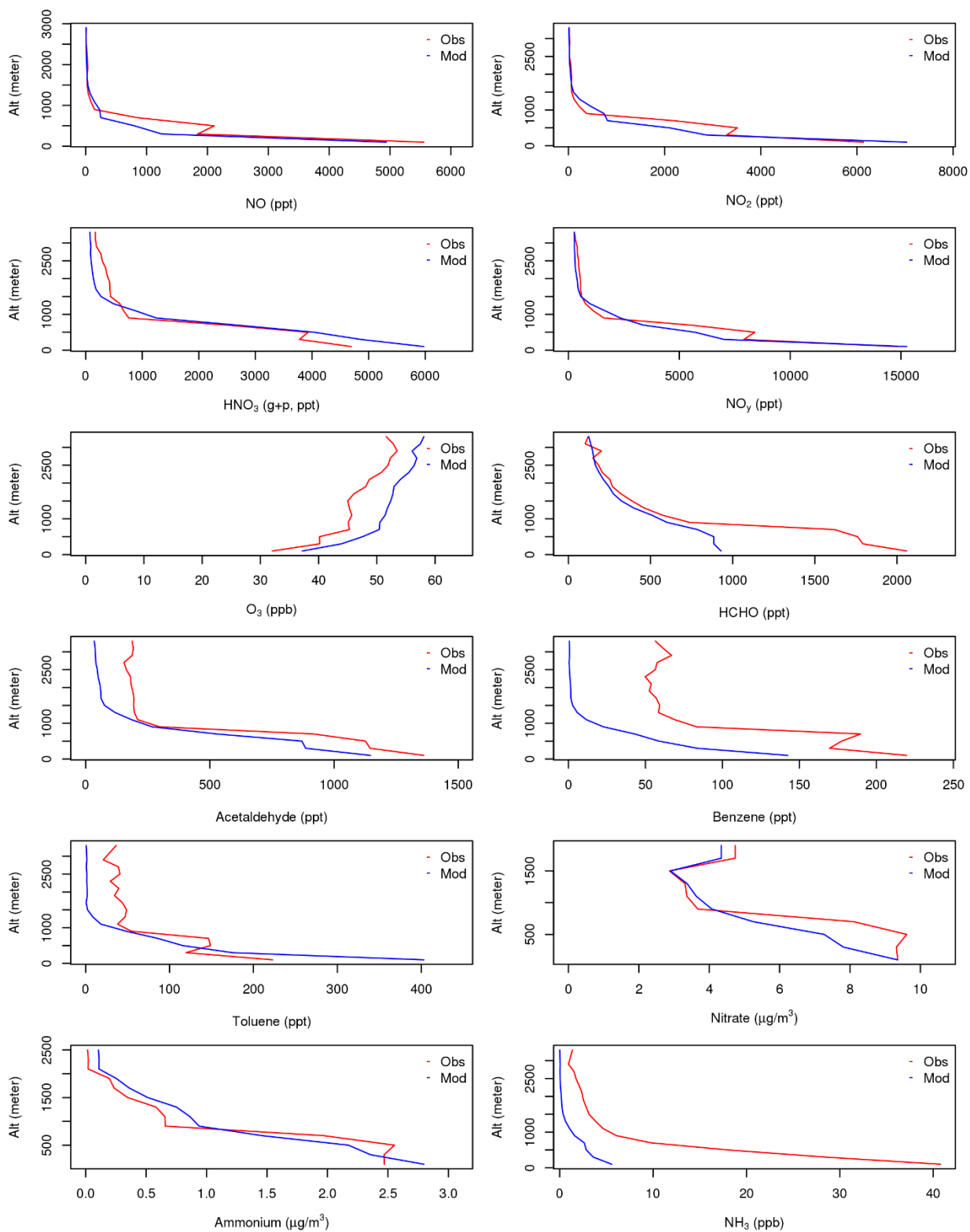
Figure S7: Comparison of observed and modeled average vertical distributions of key species based on NASA P3B flight on Jan 18.

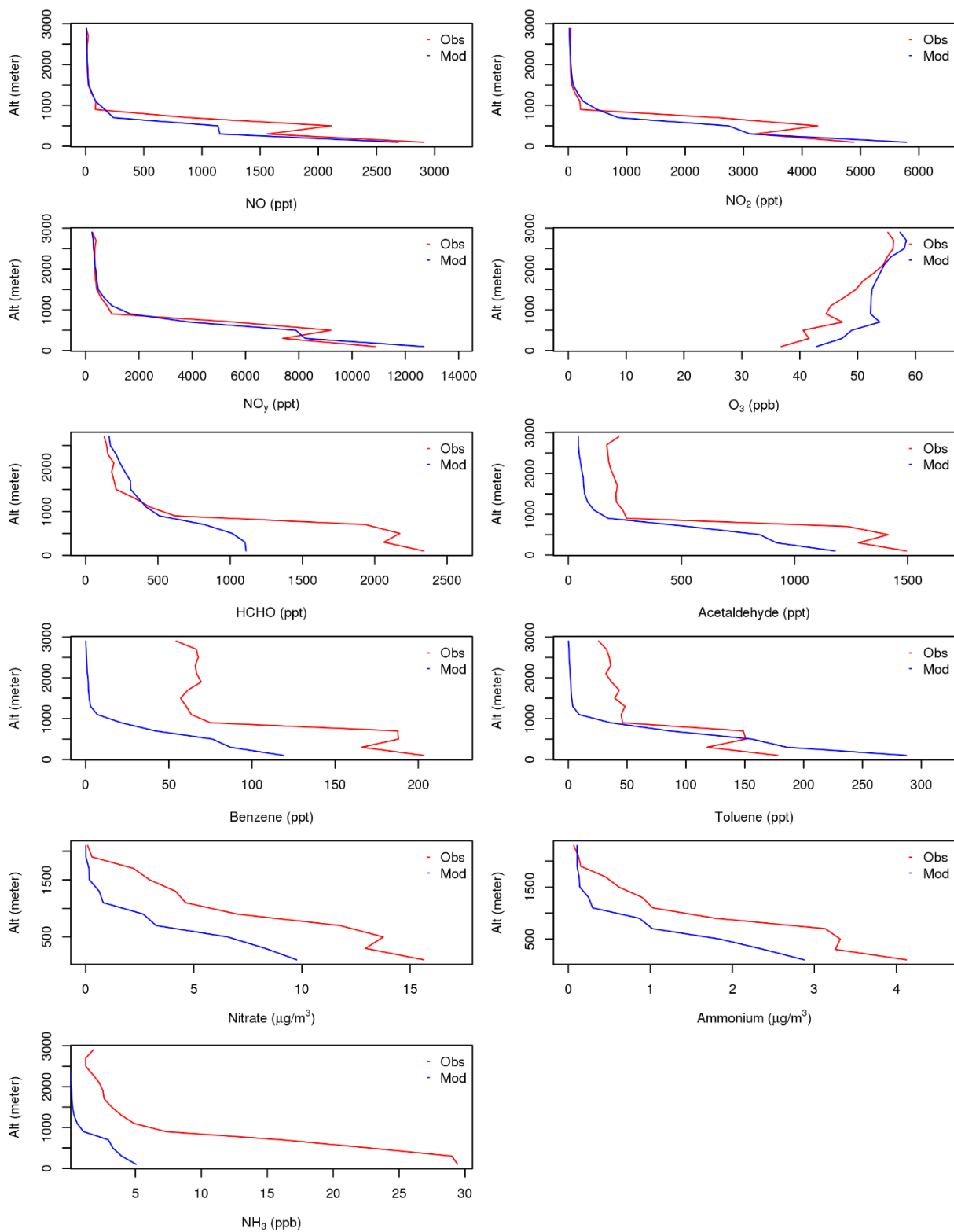


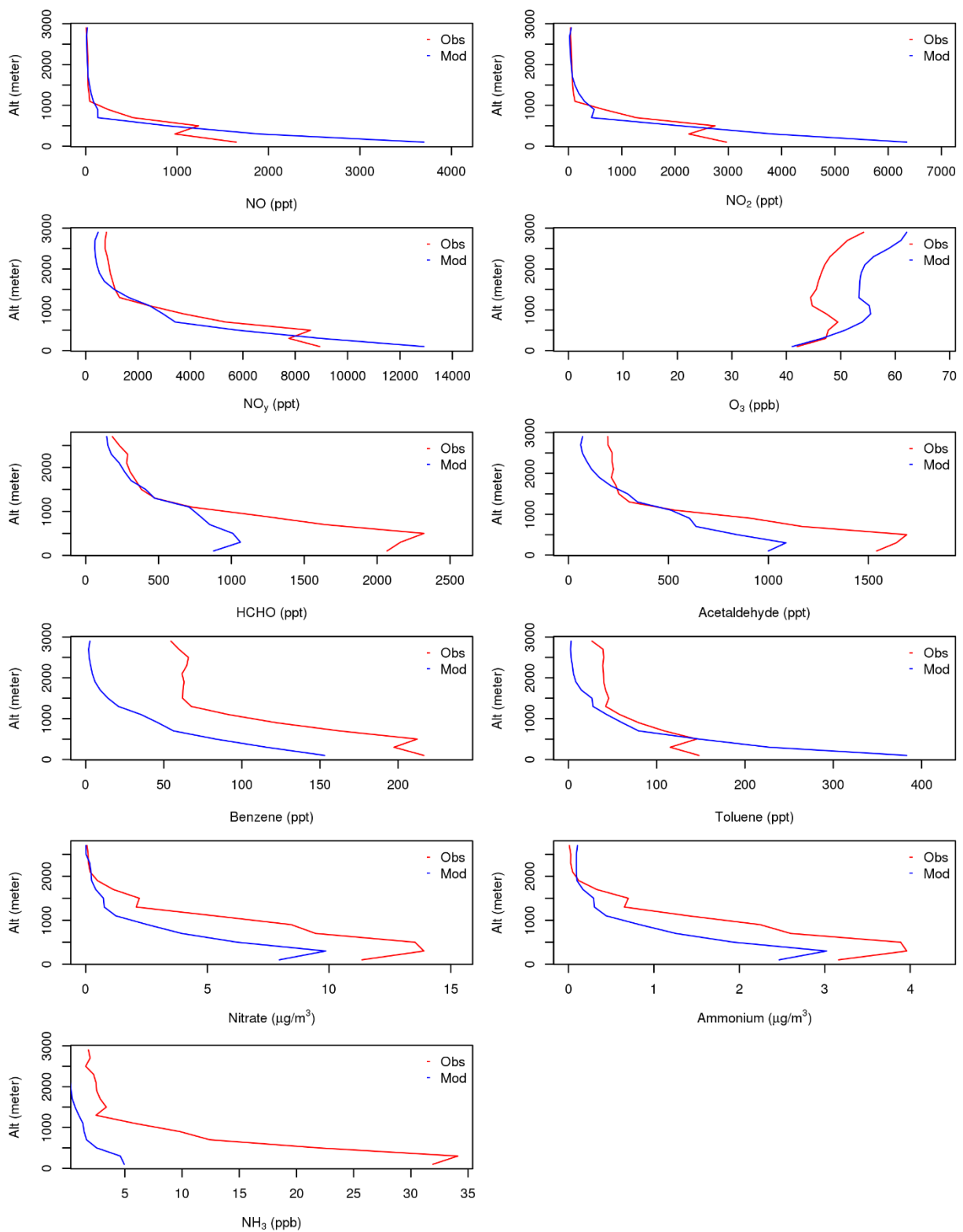




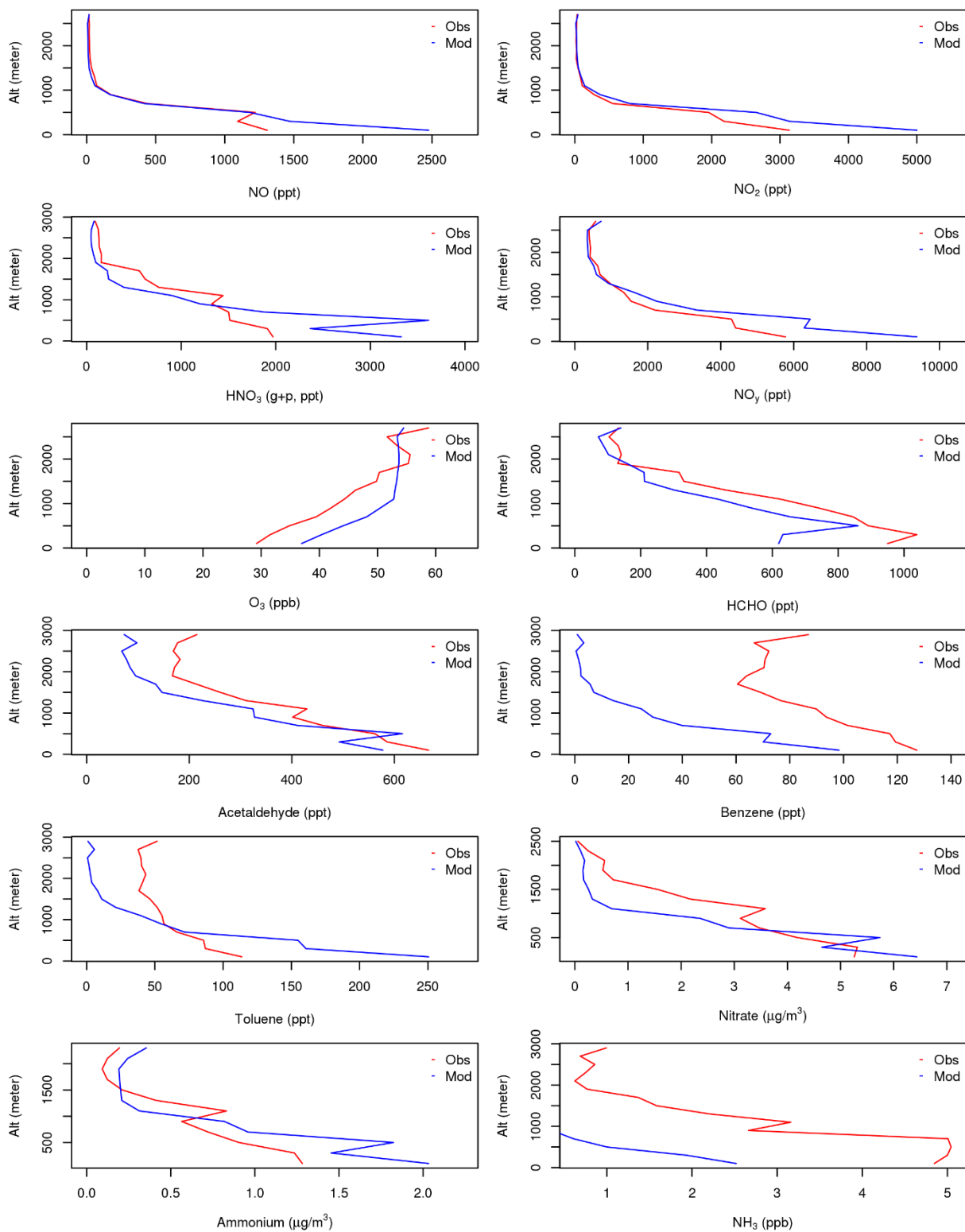












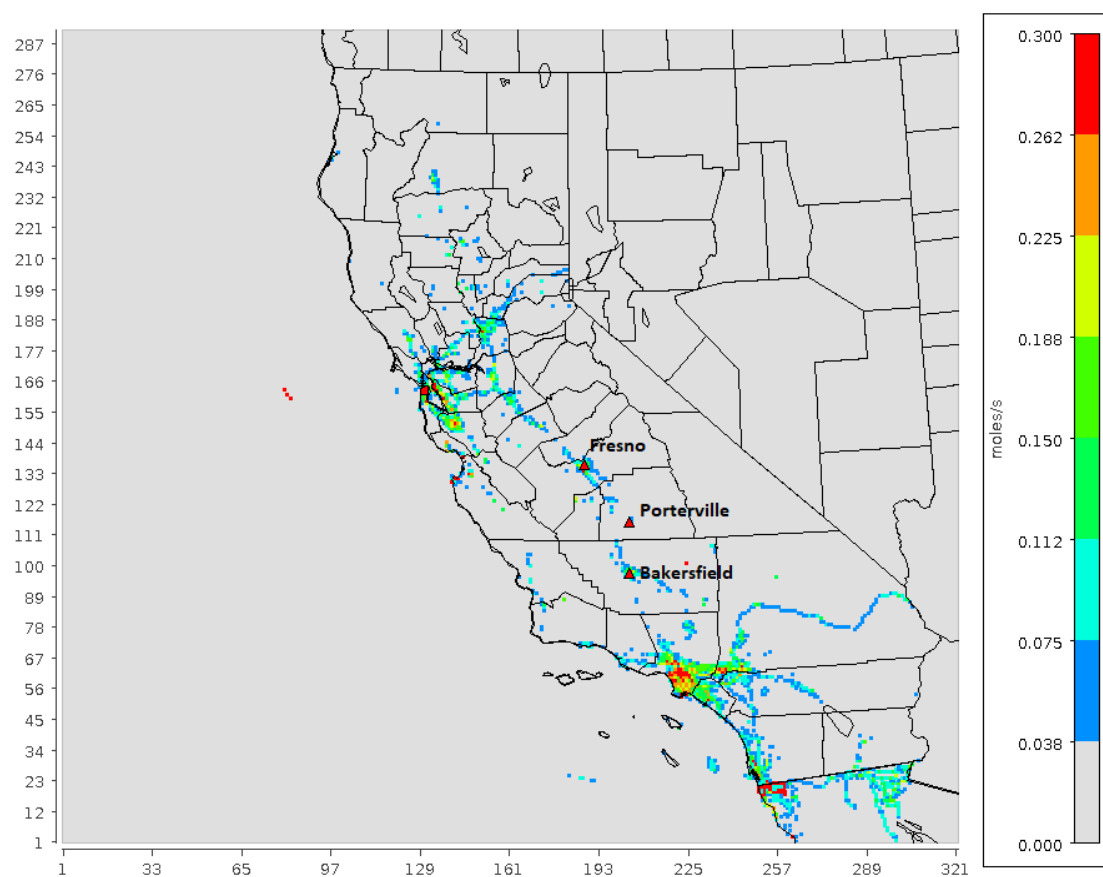


Figure S15: Spatial map of NO<sub>x</sub> emissions on Jan 20, 2013.

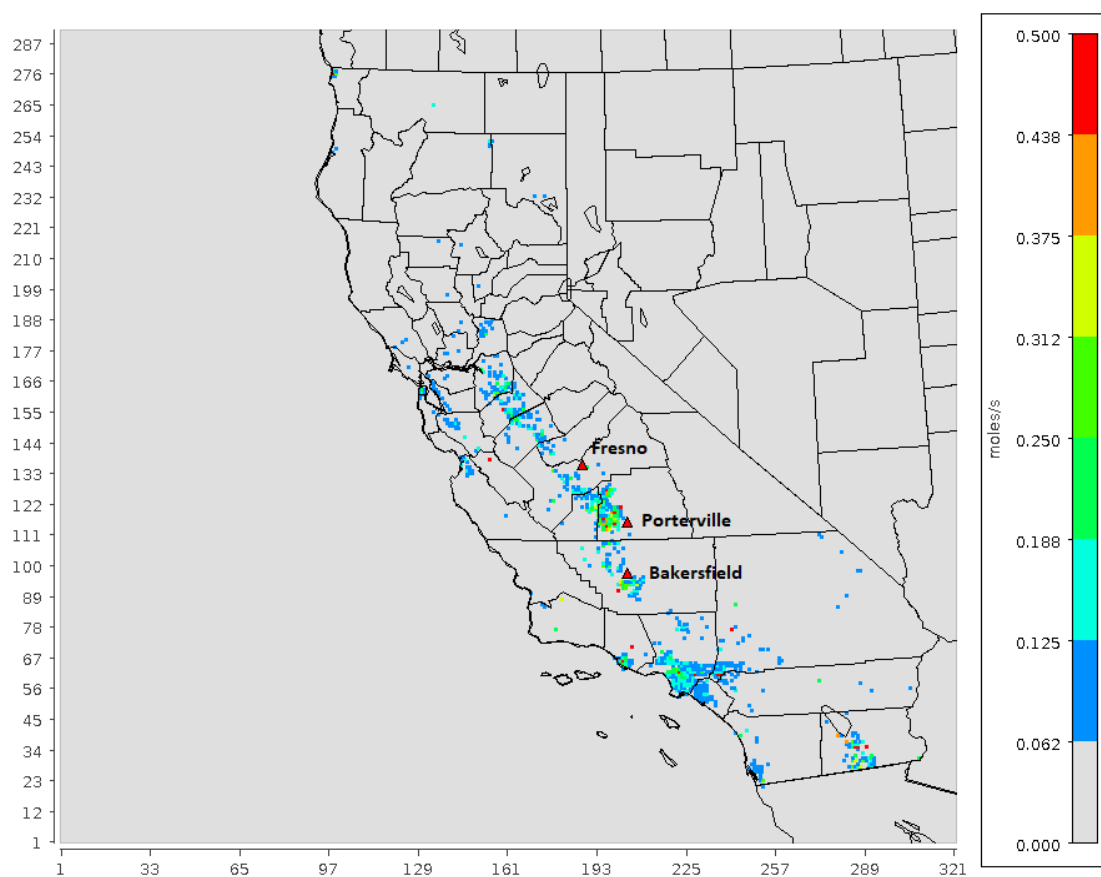


Figure S16: Spatial map of  $\text{NH}_3$  emissions on Jan 20, 2013

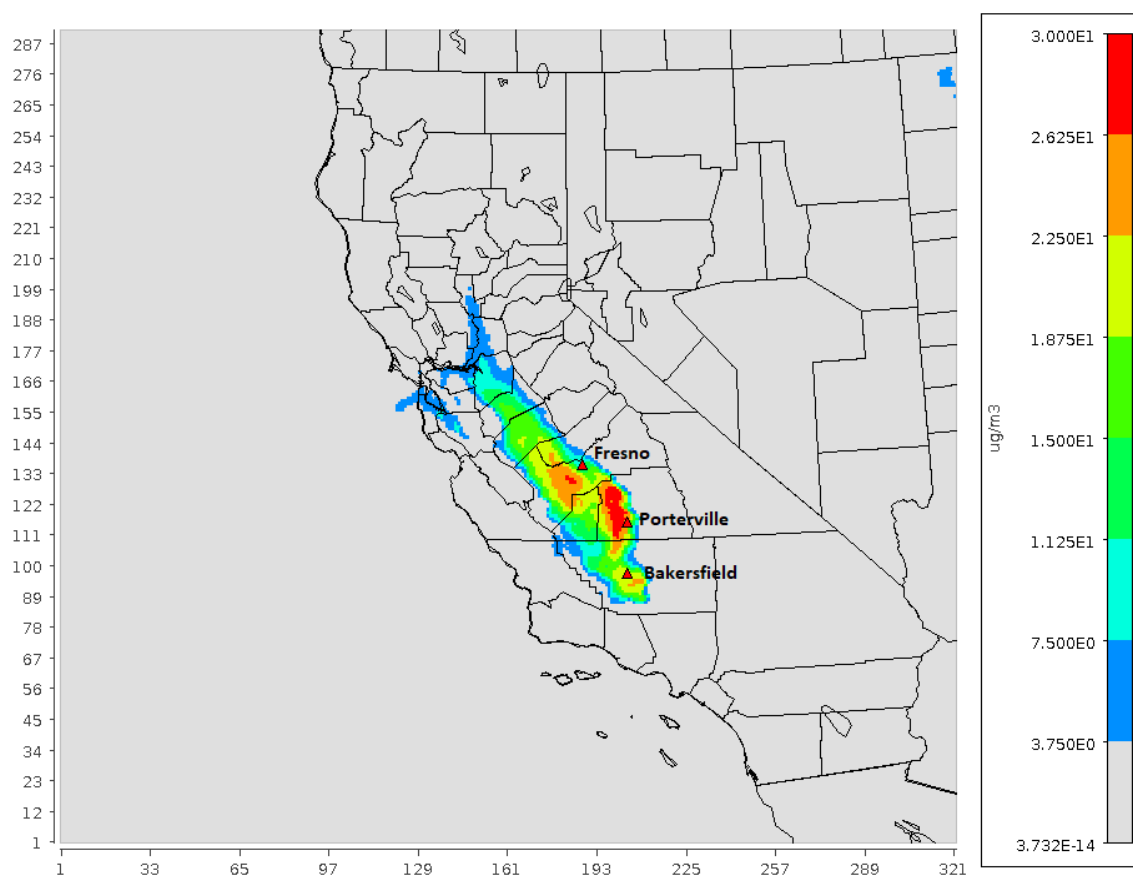


Figure S17: Spatial distributions of 24-hour average model predicted nitrate concentrations on Jan 20, 2013.

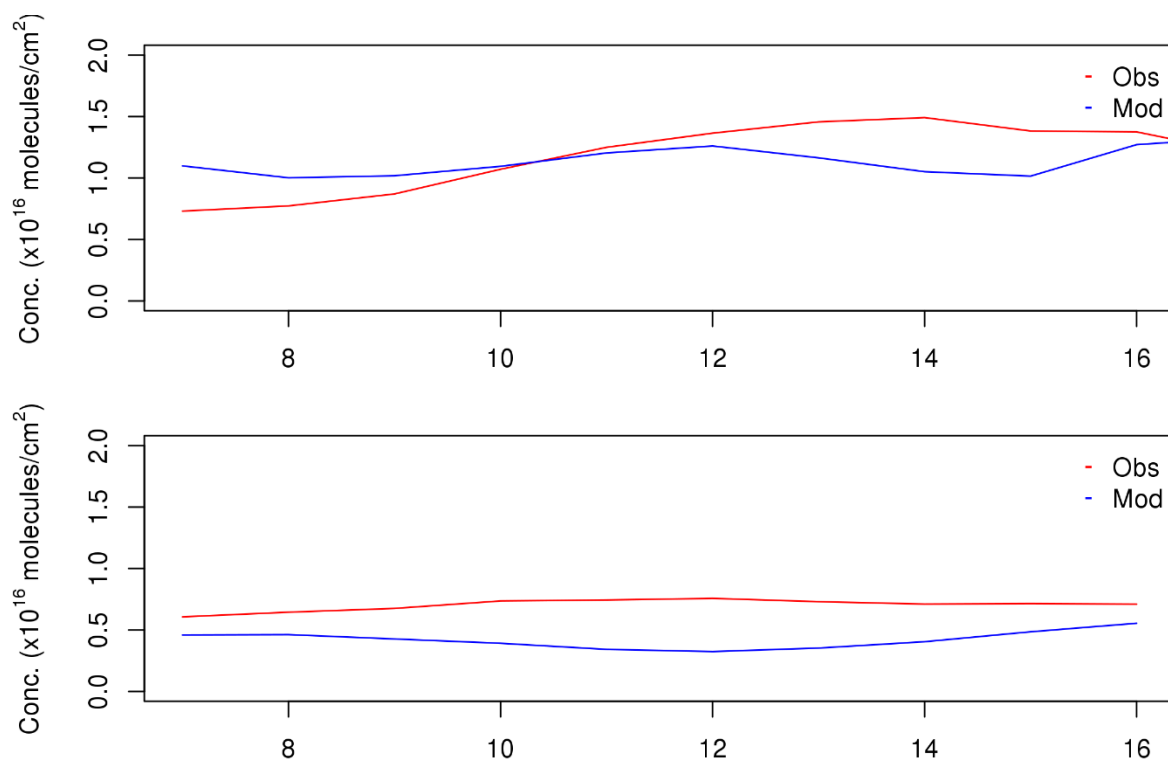


Figure S18: Comparison of diurnal profiles of observed and modeled NO<sub>2</sub> column concentrations at Fresno (top) and Porterville (bottom).